

EVALUATION OF A NOVEL THERMAL IMAGING SYSTEM FOR THE DETECTION OF
CROP WATER STATUS IN A RANGE OF MODERN COTTON CULTIVARS IN THE
SOUTHEASTERN US

By

STEFANO GOBBO

(Under the Direction of John L. Snider)

ABSTRACT

Canopy temperature has been demonstrated to be an accurate indicator of plant water status even in the humid Southeastern US. Several studies investigated the relationship between thermal image-based Crop Water Stress Index and physiological parameters as leaf water potential. However, these technologies usually rely on point measurements or have low area coverage which limit the application to commercial fields. The main objectives of this study were: (1) validate a novel thermal camera system, using well-established crop water status sensing methods and (2) calculate CWSIs from camera-derived canopy temperatures and relate them to established IRT-based CWSIs and crop physiological responses. A camera-specific well-watered baseline was defined and a strong relationship between SentinelTM-based CWSI and SmartCropTM-based CWSI ($R^2 = 0.84$) suggested the system could be used to accurately define crop water status. In addition, a linear relationship was found between SentinelTM-based CWSI and root zone soil water deficit ($R^2 = 0.59$).

INDEX WORDS: crop water stress index, leaf water potential, variable-rate irrigation, irrigation management zones.

EVALUATION OF A NOVEL THERMAL IMAGING SYSTEM FOR THE DETECTION OF
CROP WATER STATUS IN A RANGE OF MODERN COTTON CULTIVARS IN THE
SOUTHEASTERN US

By

STEFANO GOBBO

Bachelor of Science, University of Padova, Italy, 2016

A Thesis Submitted to the Graduate Faculty of The University of Georgia in Partial Fulfillment
of the Requirements for the Degree

MASTER OF SCIENCE

ATHENS, GEORGIA

2018

© 2018

Stefano Gobbo

All Rights Reserved

EVALUATION OF A NOVEL THERMAL IMAGING SYSTEM FOR THE DETECTION OF
CROP WATER STATUS IN A RANGE OF MODERN COTTON CULTIVARS IN THE
SOUTHEASTERN US

By

STEFANO GOBBO

Major Professor: John L. Snider

Committee: George Vellidis
Francesco Morari

Electronic Version Approved:

Suzanne Barbour
Dean of the Graduate School
The University of Georgia
December 2018

DEDICATION

Whereof one cannot speak,
Thereof one must be silent”

Ludwig Wittgenstein

ACKNOWLEDGEMENTS

I would like to thank the US-Israel Binational Agricultural Research and Development (BARD) Fund for providing the financial support for the project. Without them, this research opportunity would not have been possible. I would also like to thank Calvin Perry and BJ Washington for managing the experimental area and irrigation in Camilla, Lola Sexton, Lorena Nunes Lacerda, and all those who helped me in data collection. Special thanks to the members of my advising committee (John L. Snider, George Vellidis, and Francesco Morari), in particular to Dr. John Snider for editing and reviewing this document, Dr. Vellidis and Dr. Morari for giving me this Dual Master's Degree opportunity. Finally, thanks to my parents, Ester, and all my friends for the support during these 18 months I have been away from Italy.

TABLE OF CONTENTS

	Page
ACKNOWLEDGEMENTS	v
LIST OF TABLES	viii
LIST OF FIGURES	ix
CHAPTER	
1 INTRODUCTION AND LITERATURE REVIEW	1
Water Deficit on Cotton Plants	3
Crop Growth Response	4
Root Development	4
Leaf area, lint yield, fiber length.....	5
Single Leaf Response.....	6
Photosynthesis.....	6
Stomatal Conductance	7
Stomatal Limitations.....	8
Non-stomatal Limitations	8
Photorespiration	9
Dark Respiration	10
Irrigation Scheduling	11
Crop Use Curve Water Balance Method	13
Pan Evaporation Data Water Balance Method	14
UGA Checkbook Method	15

Advanced Environmental Approaches-Smart Irrigation Cotton App.....	16
UGA Smart Sensor Array	18
Plant-based Methods: Direct Methods.....	21
Minimum Leaf Water Potential	21
Predawn Leaf Water Potential	22
Plant-based Methods: Indirect Methods	24
Stem Diameter	24
Infrared Canopy Temperature.....	26
Rationale	38
References.....	39
2 VALIDATION OF A NOVEL THERMAL IMAGING SYSTEM FOR COTTON	
IRRIGATION SCHEDULING IN THE SOUTHEASTERN USA	50
Abstract.....	51
Introduction.....	52
Material and Methods	55
Results and Discussion	65
References.....	72
Figure Captions.....	76
Tables	79
Figures.....	81
3 CONCLUSIONS.....	92

LIST OF TABLES

Table 1.1 Checkbook method suggested irrigation rates	15
Table 1.2 Summary of wet and dry baselines types used for water status estimation	30
Table 1.3 Leaf Water Status classes for water status mapping in Israel	36
Table 2.1 Irrigation, Rainfall and number of irrigation events	79
Table 2.2 Total solar radiation, average IPAR, $IPAR_{tot}$, DW and RUE	80

LIST OF FIGURES

Figure 1.1 Kc curve from the Cotton App	16
Figure 1.2 User interface of the UGA SSA website, node positions and SWT graphs	19
Figure 1.3 Relationship between net photosynthesis and predawn leaf water potential	23
Figure 1.4 Actual and recommended stem growth for cotton grown in Israel	25
Figure 1.5 Actual and recommended stem daily maximum contraction for cotton.....	26
Figure 1.6 Canopy-air temperature to VPD graph.....	31
Figure 1.7 CWSI to predawn leaf water potential, and CWSI to lint yield relationships.....	35
Figure 2.1 Daily Maximum and Minimum air temperature and precipitation	81
Figure 2.2 Daily deep soil water tension weighted averages and RZSWD	82
Figure 2.3 Pre-dawn and midday leaf water potential	83
Figure 2.4 Average height, mainstem nodes, and IPAR.....	84
Figure 2.5 Net photosynthesis, stomatal conductance to water vapor, and WUE.....	85
Figure 2.6 Leaf temperature, leaf – air temperature, leaf to air VPD	86
Figure 2.7 Canopy – Air temperature differences to vapor pressure deficit (VPD) for SmartCrop™ IRTs and Sentinel™ thermal camera	87
Figure 2.8 SmartCrop-based 2018 vs Chastain et al. (2016) baselines	88
Figure 2.9 Sentinel-based Idso CWSI vs Root Zone Soil Water Deficit.....	89
Figure 2.10 Sentinel-based vs SmartCrop-based Idso CWSI.....	90
Figure 2.11 Different CWSIs calculated for SmartCrop and Sentinel.....	91

CHAPTER 1

INTRODUCTION AND LITERATURE REVIEW

The future of agriculture will likely be limited by water availability. Agriculture in the United States is a major user of water, accounting for approximately 48 percent of the total national water use. Agriculture, however, accounts for approximately 80 to 90 percent of U.S. consumptive water use due to the quantity of water removed via evapotranspiration. In Europe, many regions depend on agriculture and the amount of water used varies from 33 percent to 80 percent in some Southern Europe areas (Spain, Greece, and Italy as major examples).

Although total water demand will increase over the coming decades (OECD estimates a global 55 percent increase by 2050), because of competition with other sectors, agriculture will face the opposite trend. A perfect example of water importance is the so called “Water War”, a long-running legal dispute between the states of Florida, Georgia, and Alabama for access to Chattahoochee-Flint River Basin water resources. Moreover, competition for water with industry is likely to increase in the coming years. Temporal rainfall distribution in the Southeastern part of the United States, even if not constant from year to year, is conducive to rainfed crop production in some years. As a reference value, for growing a crop like cotton in the Southeastern US, around 46 cm are required during the entire cycle to reach the maximum yield. Obviously, production regions with much higher reference ET such as the desert Southwest, require much more water during the growing season. Considering all these aspects, and the detrimental effects of global climate change such as increased frequency and severity of unexpected rainfall and drought events on crop production, the ability to increase agricultural water use efficiency using advanced

scheduling strategies will be one of the most important challenges for the future of agriculture. Proper irrigation timing is essential to 1) limit yield losses due to water stress (deficit or excess), 2) maximize water use efficiency/economic productivity, and 3) reduce negative environmental impacts of excessive irrigation, particularly nutrient and pesticide leaching that may impact water quality.

At the crop level, evaluation of water stress responses is essential to better schedule irrigation. Water stress is manifested in two ways: (1) Drought stress, which is the most important and common one during the growing season, is caused by the lack of water within the soil profile explored by crop roots; (2) Waterlogging stress, which is caused by soil water content being close to or at saturation. However, waterlogging is a much rarer condition and is usually limited to portions of a field with low elevation, drainage problems or precipitation events where rainfall rate is higher than infiltration rate for a given area.

Variable rate irrigation (VRI) employs the concept of irrigation management zones (IMZs). An IMZ is an area of the field in which its characteristics (in terms of soil electrical conductivity, yield response, elevation, soil type, etc.) are “statistically different” from other areas of the same field. In the common VRI system, each zone is irrigated differentially. Currently, the system applies a constant rate of water for each zone throughout the season and does not consider changes in soil or plant-related factors that alter the boundaries of zones with different evapotranspiration rates. This is called static VRI.

Identifying the remote sensing technologies that most accurately reflect crop water status will allow for dynamic VRI to be applied. Dynamic Variable Rate Irrigation is a variable rate irrigation system in which the irrigation rates can be changed during the crop growing season to account for changing IMZ boundaries in order to deliver irrigation most efficiently while

mitigating crop stress. Different approaches to quantifying crop water status have been investigated in recent years and range from soil water tension measurements to leaf water potential, and many others. Utilizing canopy temperature-based approaches to alter irrigation zones and only apply water when the crop needs it represent a promising tool to maximize water use efficiency. However, extensive validation of up-and-coming thermal imaging technologies via ground-based assessments of crop water stress is needed prior to deployment of these technologies in large-scale agricultural production.

Water deficit effects on the cotton plant

Water deficit is one of the most detrimental factors for crop production in all agricultural areas and changing world climatic trends will likely increase the frequency of the severity of drought events. Generally, water deficit stress in plants is defined as the point where the plant water potential and turgor pressure are low enough to limit or inhibit normal plant processes (Hsiao, 1973). In particular, the lower the turgor pressure, the lower the force a plant can exert for cell expansion. Moreover, the severity of water stress is influenced by a combination of the duration of the stress, the growth stage when the stress occurs, and the intensity of the stress event (Snider et al., 2015a). Depending on the crop, water deficit can impact plant development to different extents and with different intensities. For cotton, water stress can affect root and shoot growth, leaf development, stem elongation, photosynthetic rate, stomatal conductance, transpiration rate, boll development, fiber quality, lint yield, and many other processes (Pettigrew 2004; McMichael et al., 2010; Snider et al., 2015a).

Crop growth responses

Root development

Soil water content is important in the formation and development of roots. Compacted soil or a soil with low water content can represent an important limitation for root proliferation (Hsiao, 1973). McMichael et al. (2010) found that rooting density increases with depth and decreases in the upper soil layers in a dry soil because plants try to maintain sufficient water uptake by exploiting water in the lower horizons. In cotton, root elongation is also maintained under water stress at water potentials below -1.5 MPa (around 35% of the maximum root elongation), whereas shoot elongation rates lower than 20% of the maximal elongation are observed at potentials smaller than -0.4 MPa (Sharp et al., 2004). Consequently, root to shoot (root/shoot) ratio increases as water availability decreases (Snider et al., 2015a).

Increased radial root resistance is one key element to limit root-to-soil outward water flux. Oosterhuis (1981) identified radial root resistance as the major factor limiting water flux; successive studies showed conflicting results for radial resistance response among different soil depths and root stages: some studies assumed radial resistance as a constant property throughout soil layers, whereas others identified different responses in roots under different growth conditions (Taylor and Klepper, 1979, Turner et al., 1987).

One of the most important aspects to consider is the ability of cotton plants to modulate water flux by means of osmotic adjustment (osmoregulation), to maintain enough turgor pressure for cell expansion (Cutler and Rains, 1977, Ackerson and Herbert, 1981, Oosterhuis and Wullschlegel 1987a). Osmotic adjustment (OA) is an adaptation mechanism to drought stress, defined as the increase in the osmotically active compatible solutes, such as sugars, inside the cells (Hsiao, 1973; Ackerson and Herbert, 1981; Sanders and Arndt, 2012). Consequently, OA increases

Ψ_s in order to maintain stable turgor pressure (Ψ_p), despite the lower water potential (Ψ_w ; Jones, 2006). In cotton, osmotic adjustment, in absolute magnitude, is greater in leaves than in roots; however, in relative terms, roots exhibit greater adjustment than leaves (this could explain the lower sensitivity to water stress of roots; Oosterhuis and Wullschleger, 1987a, b; Snider et al., 2015a).

Additionally, nitrogen availability can increase cotton tolerance to short-term drought stress periods, due to higher antioxidant production and decreased membrane damage in roots (Liu et al., 2008; Snider et al., 2015a). Considering soil temperature effects on root development, cooler temperatures have been shown to decrease root hydraulic conductance in cotton, probably also affecting water uptake (Bolger et al., 1992).

Leaf area, lint yield, fiber length

Leaf area development is important for cotton growth, increasing or decreasing the active photosynthetic surface available to intercept solar radiation. Several studies have shown canopy expansion as strongly influenced by drought stress, in particular by decreasing both the total leaf area and leaf number on sympodial (fruiting) branches. Rosenthal et al. (1987) observed decreased leaf extension rate in glasshouse cultivated cotton at available water content lower than $51 \pm 15\%$. In addition, a strong relationship between leaf area [cm^2] and boll weight [g] has been presented by Oosterhuis and Wullschleger (1988).

Therefore, lint yield is decreased mainly because of the poor source strength (defined as area x photosynthetic rate) of stressed plants, and the consequent decrease in vegetative and sympodial nodes (Krieg and Sung, 1986, Loka and Oosterhuis, 2012). Although flowers are protected from drought stress and abscission, bolls are most susceptible to abscission during the

first two weeks after flowering under water stress due to possible changes in hormone balance. In addition, right before flowering, small cotton floral buds (called squares) are extremely sensitive to drought stress and this can lead to bud abscission (Loka and Oosterhuis, 2012; Snider et al., 2015a).

Fiber thickness and length seem to respond to water stress depending on the stage of fiber development. Pettigrew (2004) showed yield was much more susceptible to drought stress than fiber quality, where significant lint yield differences were observed between dryland and well-watered crops. Moreover, Grimes and Yamada (1982) observed a negative relationship between LWP and fiber yield or length, with decreased fiber length and weight at midday leaf water potential lower than -2.8 MPa.

Single leaf responses

Photosynthesis

Water stress also affects net photosynthesis (A_N): the total amount of carbon fixation during photosynthesis *minus* the rate of carbon dioxide lost during respiration (dark respiration). The first and most intuitive effect of drought stress is a decreased whole-plant photosynthesis because of limited plant growth and, therefore, leaf area. However, photosynthesis measurements have been shown to not be as sensitive to moderate drought stress and some other parameters, such as stomatal conductance, should be investigated (Turner et al., 1986). Even though a substantial amount of literature describes water stress effects on photosynthesis, the identification of the mechanism of photosynthetic inhibition is still debated (Flexas and Medrano, 2002; Massacci et al., 2008; Snider et al., 2014; Chastain, 2015).

The two mechanisms most often considered are: (1) non-diffusion related mechanisms (enzymatic processes or other metabolic limitations), usually defined as non-stomatal limitations; (2) limitations of CO₂ diffusion to the carboxylation site, defined as stomatal limitations. Stomatal limitations are considered the main photosynthesis-limiting factor under moderate drought stress, but non-stomatal limitations are observed under more severe stress (Ennahli and Earl, 2005; Snider et al., 2015a). Stomatal and non-stomatal limitations are briefly explained below.

Stomatal conductance

Stomatal conductance to water vapor (g_s) is defined as the measure of the water vapor exiting through the leaf stomata and is one of the first and most important noticeable parameters indicating water stress in several plants. Plants tend to close stomata during a drought stress period in order to limit the amount of water lost, and by doing this, stomatal conductance is generally decreased. In addition, several factors influence stomatal conductance, including phytohormone levels, leaf water potential, air temperature, air moisture content (or relative humidity), and leaf growth stage. Stomatal conductance has been found to be negatively correlated with vapor pressure deficit (VPD, the difference between vapor pressure at saturation and the amount of water vapor present in the air at a certain time) in several plants ranging from tree crops to common row crops (Dang et al., 1997; Day, 2000; Diaz, 2013; Chastain, 2015). Considering leaf water potential, cotton stomata have been shown to stay open even under drought stress at leaf water potential up to -3MPa (Ackerson et al., 1977). For abscisic acid, a well-documented mechanism has been presented indicating ABA synthesis in the root and subsequent movement of ABA to the leaves through the xylem in response to drought stress causes declines in g_s (Davies et al., 1991). However, some split pot studies in cotton where half of the root system was maintained under wet

conditions and the other half was allowed to dry, concluded stomatal conductance was unaffected by drying treatments (White and Raine, 2009).

Stomatal limitations

An increase in drought stress decreases stomatal conductance and CO₂ concentration inside the leaf and at the carboxylation site of Rubisco (RuBP carboxylase/oxygenase), decreasing net photosynthesis (Medrano, 2002). However, the CO₂ concentration within the leaf (C_i) cannot be considered a precise estimation of the CO₂ concentration at the carboxylation site (C_C), and usually leads to an overestimation of CO₂ concentration, for different reasons: the first one is the wrong assumption that CO₂ and water vapor diffuse only through stomata (in fact, during drought stress water vapor can diffuse also through the cuticle because of the lower cuticle resistance to water vapor diffusion than for CO₂ diffusion); the second reason is the uneven stomatal closure during drought stress which can generate C_i overestimation (Long and Bernacchi, 2003; Ennahli and Earl, 2005). Nevertheless, cotton has been demonstrated to evenly respond in terms of stomata closure to water stress (Massacci et al., 2008).

Non-stomatal limitations

In addition to stomatal limitations, there are situations where non-diffusional mechanisms limit photosynthesis under drought stress. There is evidence that the activity of carbonic anhydrase (for HCO₃⁻ conversion), Rubisco (or RuBP) concentration or activity, or decreased ATP (adenosine triphosphate) synthesis because of limited photophosphorylation under low leaf water potential constrains photosynthesis (Jones, 1973; Tezara et al., 1999; Lawlor and Tezara, 2009). Considering Rubisco activity inhibition, several studies demonstrated the possible dependence of

this decline on high temperatures (T_{leaves} around 37-40 °C) more than on water deficit conditions (Carmo-Silva et al, 2012). In addition, ATP synthesis reduction because of drought stress has not been highly investigated in cotton. Finally, photosystem II and the electron transport rates through photosystem II (ETR), if evaluated between 1200 and 1500 h, are either unaffected or increased under moderate water stress (Snider et al., 2013; Chastain et al., 2014; Snider et al., 2015a) for field-grown cotton.

Considering scientific works on stomatal and non-stomatal limitations, photosynthesis is mainly limited by CO₂ diffusion to the carboxylation site (diffusional mechanisms) under moderate drought stress conditions, whereas, under severe drought stress, metabolic (non-diffusional) limitations become important and lead to decreased carboxylation efficiency. To support these last two points, it is important to consider net photosynthesis recovery from moderate/severe stress conditions. Upon rewatering of moderately stressed plants, net photosynthesis (A_N) returns to pre-stress levels. On the contrary, rewatering severely stressed plants causes the CO₂ concentration at carboxylation site to return to pre-stress levels, but not A_N , because of the lasting non-stomatal limitation effect. Photosynthetic rate response to C_i (A_N/C_i curves) or C_c (A_N/C_c curves) have been used to detect whether a plant's photosynthetic rate was able to return to pre-stress levels when CO₂ concentration at the carboxylation site was artificially maintained at levels comparable to well-watered plants (Ennahli and Earl, 2005).

Photorespiration

Photorespiration (P_T) is an oxidative photosynthetic carbon cycle (C₂ photosynthesis) defined as the oxygenation reaction of Rubisco (oxygen combined with RuBP, instead of the desired reaction in which carbon dioxide is added to RuBP), resulting in a limited carbon

assimilation in stress periods such as drought stress and high temperatures. In photorespiration, oxygen + RuBP produces an unstable 5 C intermediate that breaks down to 3-phosphoglycerate + glycolate. Every 2 oxygenation reactions produce 2 glycine which undergo a decarboxylation reaction in the mitochondria to produce serine + CO₂, resulting in a net carbon loss and decreasing efficiency of photosynthesis (Taiz and Zeiger, 2010). Different studies suggest different responses of photorespiration: in some cases, water deficit leads to decreased photorespiration rate and decreased photochemical responses such as a decrease in photosynthetic electron transport rate (Flexas et al., 1999; Zhang et al., 2011). Some others have shown increased P_r under drought stress (Cornic and Fresneau, 2002; Massacci et al., 2008). In addition, some plants showed no photorespiration changes, probably due to some adaptation mechanisms to water stress.

In cotton, studies showed different responses in terms of photorespiration. P_r has been shown to both increase or decrease under water stress conditions (Perry et al., 1983; Massacci et al., 2008). Some authors suggest, high photorespiration and ETR values limit reactive oxygen species formation by serving as an electron sink during stress (Kitao and Lei, 2007).

Dark respiration

Dark respiration (R_D) is defined as the respiration process that occurs even without the presence of light. R_D has a biphasic response to drought stress, with (1) a decrease under moderate drought stress conditions and (2) a subsequent R_D increase under severe drought stress (Pallas et al., 1967; Flexas et al., 2005). This likely explains why several scientific works showed either decreased or increased dark respiration rates because of drought stress (Loka et al., 2011; Zhang et al., 2011; Chastain, 2015). Where plant water status was tightly controlled, Snider et al. (2015b) found a linear relationship between predawn water potential (Ψ_{PD}) and predawn respiration (R_{PD}),

and the greater drought stress sensitivity of R_{PD} compared to other photosynthetic processes. This suggests differences in drought stress evaluation (time, intensity, and other aspects) could partially explain the different R_D responses.

Irrigation scheduling

Irrigation is the ability to distribute the required amount of water to agricultural crops at needed intervals. The main benefits derived from irrigation are the stabilization of crop production, especially during dry years, and a better nutrient use efficiency due to higher yields. Irrigating a field does not necessarily mean increasing production. In fact, Vories et al (2006) observed improper irrigation timing can result in yield losses between 150 and 750 \$/ac. Moreover, a common behavior among farmers is to start irrigating after some visual signs of drought stress are observed (i.e. wilted plants, Snider et al., 2016).

Although the proportion of irrigated area to total agricultural area is continuously increasing in Europe and in the United States (USDA, 2013 Farm and Ranch Irrigation Survey; Eurostat, 2016 Agriculture, forestry and fishery statistics), the amount of farmers adopting “technological” irrigation scheduling tools, such as using soil moisture sensors or remote sensing techniques, is still low (soil moisture sensors are used for scheduling irrigation in 11% of the total US farms and in 9% of total farms in the State of Georgia, for European countries precise data are not available, but the adoption of these methods seems much lower). Commonly used irrigation scheduling methods such as basing decisions on the “feel of soil”, visual crop condition, or a pre-determined irrigation calendar (1 irrigation per week as an example), are extremely linked to the farmer’s subjective evaluations. Importantly, irrigation based on visible signs of drought stress can penalize yield, representing an inefficient irrigation scheduling approach (Perry and Barnes, 2012;

Snider et al., 2016). Moreover, to define when and how much to irrigate, reliable thresholds must be used as a reference. This process is called irrigation scheduling and the types of irrigation triggers commonly used can be divided into two broad categories: (1) environmental factors, such as days after the last rainfall event, soil water holding capacity, and water balance approaches that account for evapotranspiration, and (2) plant-based measures, indirect or direct measures of crop water status (Snider et al., 2016).

Among environment-derived irrigation scheduling methods, the first and most adopted is the water balance approach (Equation 1).

$$ET_c = P_e + I + C + \Delta S - D \quad (1)$$

In the equation, water additions (precipitation input, P_e ; capillary contribution, C ; and irrigation I) are subtracted from water losses (evapotranspiration, ET_c and water percolation, D). The difference is represented by ΔS as the change in root zone soil water storage. Generally, the equation can be simplified in soils with minimal compaction, high water infiltration, and limited surface runoff, as the simple difference between evapotranspiration (ET_c) and precipitation (P_e ; Equation 2). This difference is supplied via irrigation (Kisekka et al., 2010).

$$I = ET_c - P_e \quad (2)$$

Evapotranspiration ET (in mm/day), is defined as the sum of water evaporation from soil and transpiration from the canopy surface. ET depends on weather variables (wind speed, solar radiation, humidity, temperature), as well as soil characteristics, cultural practices, and crop

characteristics (Fisher and Udeigwe, 2012). ET_c for a given crop is estimated using the following formula: ET_c (crop evapotranspiration) = ET_0 (reference evapotranspiration) x K_c (cultural coefficient). ET_0 is the evapotranspiration observed from a well-watered, uniformly-covered grass field (Equation 3; Allen et al., 1998; Zotarelli et al., 2010).

$$ET_0 = \frac{0.408\Delta (R_n - G) + \gamma \frac{900}{T + 273} u_2 (e_s - e_a)}{\Delta + \gamma(1 + 0.34 u_2)} \quad (3)$$

where ET_0 is the reference evapotranspiration rate (mm d^{-1}), R_n is the net radiation at the crop surface ($\text{MJ m}^{-2} \text{d}^{-1}$), G is the sensible heat flux into the soil ($\text{MJ m}^{-2} \text{d}^{-1}$), T is the mean daily air temperature at 2 m ($^{\circ}\text{C}$), u_2 is the wind speed at 2 m, e_s is the saturation vapor pressure (kPa), e_a is the actual vapor pressure (kPa), Δ is the slope of the vapor pressure curve ($\text{kPa } ^{\circ}\text{C}^{-1}$).

ET_c is evaluated using lysimeters, which measure water gain or loss during the entire day. Once ET_0 and ET_c are known, K_c can be calculated simply as ET_c / ET_0 . ET_c and K_c values are crop specific and change throughout the season.

Two different water balance approaches are commonly used: crop use curves or pan evaporation data (Harrison, 2009). The application of the crop use curve and pan evaporation approaches are explained below with examples (Harrison, 2009).

Crop Use Curve Water Balance Method

Assuming 24 cm as the rooting depth, information on soil water holding capacity (WHC, the difference between field capacity, FC and permanent wilting point, PWP) can be obtained from the soil conservation guide of the local Soil Conservation Service. In the following example, a WHC value of 5 cm is assumed.

1. From the crop curve, identify daily use rate (in cm per day).
2. Define a lower limit for soil water depletion (for example 50 percent of the WHC, $5 \text{ cm} \times 0.5 = 2.5 \text{ cm}$ to be replaced). Considering an irrigation efficiency of 70%, the amount to be replaced is $2.5 \text{ cm} / 0.7$ (irrigation efficiency) $\approx 3.6 \text{ cm}$.
3. The irrigation frequency is defined by dividing the amount of water to be replaced (2.5 cm) by water use per day (from crop curve, 0.8 cm/day). The irrigation frequency is calculated as $2.5 \text{ cm} / 0.8 \text{ cm day}^{-1} \approx 3$ days. Thus, considering the irrigation efficiency of the system (70%), it is necessary to apply 3.6 cm (instead of 2.5 cm) every 3 days to fill the soil profile.

Pan Evaporation Data Water Balance Method

To demonstrate the pan evaporation method, water holding capacity is defined as before (in this case, for the selected rooting depth, WHC = 4 cm). A pan evaporation rate (available from weather stations) of 0.7 cm day^{-1} is used.

1. The crop coefficient (K_C), from the crop coefficient curve, is 1.1.
2. Calculate daily water removal by multiplying the crop coefficient x pan evaporation rate ($1.1 \times 0.7 = 0.77 \text{ cm day}^{-1}$).
3. Define a maximum allowable water depletion (for example 50 percent of WHC, $4 \text{ cm} \times 0.5 = 2 \text{ cm}$ to be replaced). If irrigation efficiency is 70%, the amount to be replaced is 2 cm (maximum allowable water depletion) / 0.7 (irrigation efficiency) $\approx 2.85 \text{ cm}$.
4. Irrigation frequency is defined by dividing amount to be replaced by water use per day = $2 \text{ cm} / 0.77 \text{ cm day}^{-1} \approx 2.6$ days. Thus, considering the irrigation efficiency coefficient, it is necessary to apply 2.85 cm every 3 days to fill the soil profile.

UGA-checkbook method:

Another simplified water balance approach is the University of Georgia’s Checkbook method. With this method, supplemental irrigation is provided to reach weekly target amounts of water (rainfall + irrigation; Table 1.1, Cotton Production Guide, Whitaker et al., 2018).

Table 1.1 Checkbook method suggested irrigation rates (Whitaker et al., 2018).

CROP STAGE	cm/week	cm/day
Week beginning at 1 st bloom	2.5	0.38
2 nd week after 1 st bloom	3.8	0.55
3 rd week after 1 st bloom	5.0	0.75
4 th week after 1 st bloom	5.0	0.75
5 th week after 1 st bloom	3.8	0.55
6 th week after 1 st bloom	3.8	0.55
7 th week and beyond	2.5	0.38

The Checkbook method is a crop stage-specific water requirement method and does not consider possible environmental effects that influence ET, such as leaf area index, temperature, relative humidity, or wind speed. In addition, using this approach for cotton, irrigation is terminated when the crop reaches 10% open boll (Cotton Production Guide, Whitaker et al., 2018).

This method has been shown to consistently produce high yields, but advanced environmental or plant-based approaches tend to result in much better yields, drastically increasing water use efficiency (WUE) (Vellidis et al., 2014; Migliaccio et al., 2016). Although the checkbook method represents an easy way to determine when and how much to irrigate, it can reduce crop yields during wet years due to overirrigation (Vellidis et al., 2016; UGA, Cotton Production Guide, Whitaker et al., 2018).

Instead of using a very basic water balance calculation, as the UGA Checkbook method does, the UGA Smart Irrigation Cotton app incorporates climatic data to calculate real time ET_C (Migliaccio et al., 2013; Vellidis et al., 2014). The Cotton App utilizes meteorological data, soil parameters, crop phenology, and K_C to estimate root zone soil water deficit, RZSWD (in inches or %). The K_C is adjusted using growing degree days (GDD) instead of days after planting (DAP), because GDD correlates to cotton growth and development much better than DAP (Figure 1.1).

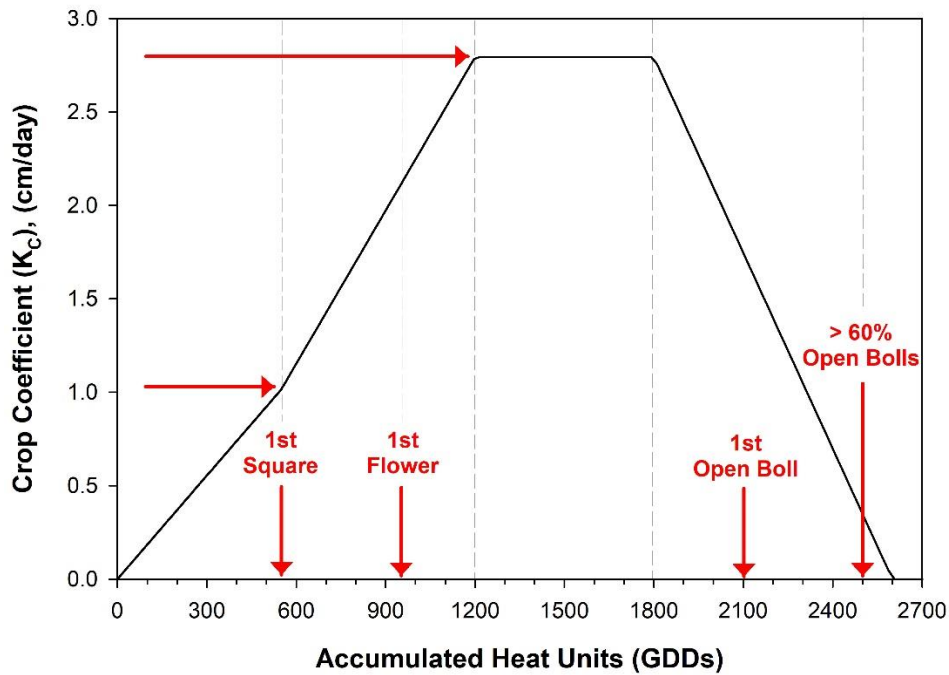


Figure 1.1. Crop coefficient (K_C) curve used from the Cotton App with the corresponding GDD-based phenological stages for cotton (Vellidis et al., 2014).

By knowing how many GDD have accumulated since planting, the Cotton App predicts what stage of growth the crop is in. Moreover, growth stage impacts water use. The following formula is used to estimate GDD (Equation 4), where T_{max} is the highest temperature of that day,

T_{min} is the lowest temperature, and T_{base} is the minimum temperature for observing plant growth, set at 15.6 °C.

$$GDD = \frac{T_{max} - T_{min}}{2} - T_{base} \quad (4)$$

Root zone soil water deficit (RZSWD, the available water content within the effective rooting depth) is calculated using USDA-NRCS soil data, considering effective rooting depth as a parameter that changes during the season as the root system develops. For cotton, the model sets the initial root depth at 15.2 cm, and then it increases by a factor of 0.8 cm/day until it reaches a value of 76 cm (Vellidis et al., 2014). For daily plant available soil water content calculations, the following water balance formula is used (Equation 5).

$$AWC_1 = AWC_0 - ET_{c0} + (P_0 + I_0) \quad (5)$$

Where AWC_1 is today's available water content, AWC_0 is yesterday's available water content, ET_{c0} is yesterday's evapotranspiration, P_0 is yesterday's precipitation, and I_0 is yesterday's irrigation amount.

The suggested irrigation threshold for cotton is set at a soil water tension value of 40 kPa or 50% RZSWD, however, the irrigation threshold really depends on soil characteristics, crop type and can be changed according to specific crop needs (Vellidis et al., 2016). The Cotton App does not automatically trigger irrigation if these thresholds are verified but only sends a notification to the user when this condition occurs. Vellidis et al. (2014) found increased cotton lint yield but

mainly increased water use efficiency by comparing the Cotton App to the Checkbook method, and similar yields and WUE comparing plant-based methods, such as canopy temperature-based CWSI, or other environmental-based methods (as Irrigator Pro), to the Cotton App.

UGA smart sensor array

The University of Georgia Smart Sensor Array (UGA SSA) is an irrigation scheduling system which makes irrigation recommendations based on soil water tension readings. Soil water tension (SWT, in kPa) is the absolute value of soil matric potential (Ψ_M) and indicates the amount of pressure required from a plant to extract water from the soil. The lower the soil matric potential (and the higher the soil water tension), the drier the soil. On the other hand, soil water tension close to 0 kPa indicates saturated conditions (Vellidis et al., 2013).

The UGA SSA system is composed of several nodes and a base station for data collection (Liakos et al., 2015; Migliaccio et al., 2016). Each node has temperature and moisture sensors, a radio board, a radio frequency (RF) transmitter, and is powered by two 1.5 V batteries. Each node incorporates 3 integrated Watermark[®] soil moisture sensors (Irrometer, Riverside, California, USA; Thomson and Armstrong, 1987; Shock et al., 1998, 2003) measuring SWT at three different depths (usually 20, 40, and 60 cm below soil surface, changeable as the investigated crop changes), and up to 2 thermocouples for soil/canopy temperature measurement. The RF transmitter is a low power and cheap 2.4 GHz radio module which sends sensor data to the base station. Nodes utilize a wireless mesh network for communication. Using this network, information “jumps” from node to node to reach the base station (Vellidis et al., 2008). This allows each node to save energy by limiting the total required transmission distance, even though the potential transmission range has been documented to exceed 750 meters (Vellidis et al., 2016). The base station, located in a

strategic position (usually at the center pivot point), is designed to receive all sensor data on a regular interval, defined by the operator (Liakos et al., 2015). Successively, the base stores the received data on a computer and sends it via cellular modem to an FTP (file transfer protocol) server.

The collected soil water tension raw data are then processed and displayed on a dedicated website (<http://ugassa.flintirrigation.com/>) using a resume map for each field with gauges indicating the actual SWT for each node and in more detail, by clicking on a specific node, using graphs with SWT trends at the three defined depths for each node, as shown in Figure 1.2 (Vellidis et al., 2016).

In addition to SWT data visualization, the UGA SSA website calculates irrigation recommendations for each irrigation management zone (IMZ). IMZs are usually defined considering soil electrical conductivity data (EC) and soil type data from the USDA-NCRS Web Soil Survey (Liakos et al., 2015; Vellidis et al., 2016).

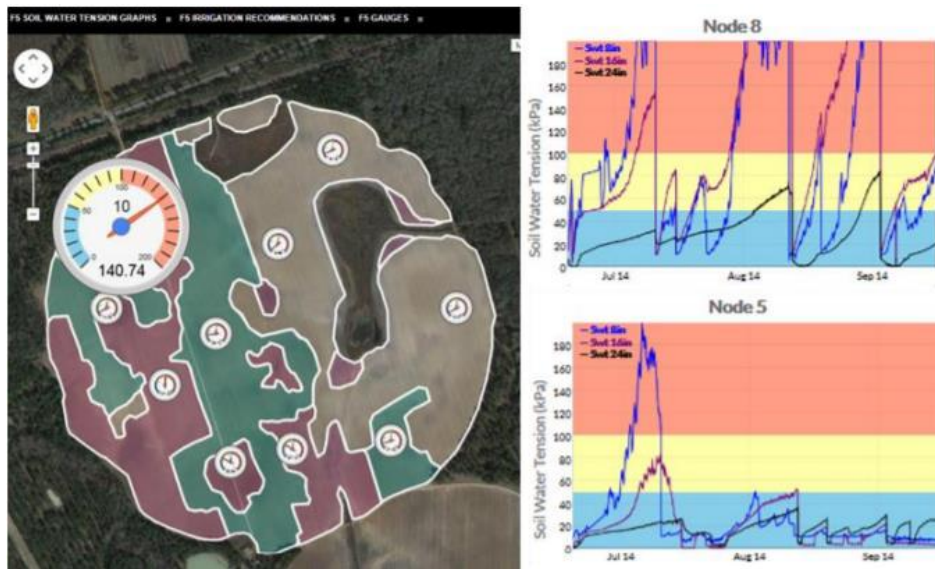


Figure 1.2 User interface of UGA SSA website, indicating node positions on the various IMZ (on the left), typical SWT readings displayed for each node (Vellidis et al., 2016)

The Van Genuchten model is used to convert SWT data into volumetric water content (VWC; Equation 6). Soil water tension values measured from 7 to 9 am at the three depths are weighted using the Equation 7 to get a unique value to be used in the Van Genuchten model (Van Genuchten, 1980; Liakos et al., 2015; Liang et al., 2016).

$$\theta(\psi) = \theta_r + \frac{\theta_s - \theta_r}{[1 + (\alpha|\psi|^n)]^{1-\frac{1}{n}}}$$
(6)

$\theta(\psi)$ is the water retention curve (l^3l^{-3})

$|\psi|$ is the suction pressure ($[l]$ or cm of water)

θ_s is the saturated water content (l^3l^{-3}), θ_r is the residual water content (l^3l^{-3})

α is related to the inverse of the air entry suction, $\alpha > 0$ (l^{-1} or cm^{-1})

n is a measure of the pore size distribution, $n > 1$

$$(0.5)(SWT_{20\text{ cm}}) + (0.3)(SWT_{40\text{ cm}}) + (0.2)(SWT_{60\text{ cm}})$$
(7)

Irrigation recommendations are finally displayed on the website for each management zone in the same way SWTs are displayed for each node. A similar free-access irrigation scheduling tool called Irrigator Pro has been developed by USDA for peanuts (Davidson et al., 2000). Irrigator Pro evaluates soil and air temperature, rainfall, and peanut physiology to provide a YES/NO decision for peanut irrigation in case the soil is too dry, or in case irrigation is required for pegging. However, Irrigator Pro does not make irrigation recommendations, it is up to the farmer to define the irrigation rates, based on experience. In pivot-irrigated peanuts, the UGA SSA system has shown to better respond in terms of yield in the wettest areas of the field, on the other hand,

Irrigator Pro has shown to better respond in sandy and high elevation areas, probably because the irrigation threshold for UGA SSA system set at 50 kPa corresponds to a much dry soil condition (Vellidis et al., 2016).

Plant based methods-Direct methods

Plant-based direct methods for scheduling irrigation are all the approaches where irrigation is triggered as a function of plant water status. The most widely used direct plant-based methods are leaf water potential measurements during different diurnal time periods: (1) during afternoon hours (approximately between 1200 and 1500 h), defined as midday or minimum leaf water potential (Ψ_{MD}) or (2) during predawn hours (approximately from 0400 to 0600 h), defined as predawn or maximum leaf water potential (Ψ_{PD}). These two methods are briefly discussed below.

Minimum Leaf Water Potential

When considering midday leaf water potential (Ψ_{MD}) changes, plants are generally divided in isohydric (plants able to maintain a stable leaf water potential when water is available, but also during drought stress by limiting transpiration with stomatal closure), or anisohydric (plants which maintain stomata open also during drought stress periods and show substantial changes in leaf water potential). Cotton is an anisohydric plant and leaf water potential measures can be used as a measure of crop water deficit conditions, and to schedule irrigation (Lacape et al., 1998; Jones, 2006). Leaf water potential is extremely dependent on the time of measurement: Ψ_L has a maximum just before sunrise, then Ψ_L declines to a minimum value between 1200 and 1500h and increases successively to a new maximum value before sunrise the next day (Grimes and Yamada 1982).

Several physiological responses to drought stress have been linked to Ψ_{MD} over the years; these include stem elongation (linear decline below Ψ_{MD} of -1.3 MPa; Grimes and Yamada, 1982), leaf expansion (Turner et al., 1986; Pettigrew, 2004), lint yield (decreased yield values at Ψ_{MD} below -1.9 MPa; Grimes and Yamada, 1982), and stomatal conductance and photosynthesis (decrease with Ψ_{MD} values below -1.9 MPa; Ennahli and Earl, 2005; Snider et al., 2013). A Ψ_{MD} value of -1.9 MPa has been used as a threshold for scheduling irrigation (Grimes and Yamada, 1982; Snider et al., 2015a).

However, Ψ_{MD} is extremely dependent on environmental factors and fluctuates because of them. In particular, cloud cover and vapor pressure deficit (VPD) have been found to impact Ψ_{MD} , and several studies have attempted to normalize Ψ_{MD} to better schedule irrigation based on Ψ_{MD} information (Grimes et al., 1987; Conaty et al., 2014, Snider et al., 2015a; Chastain et al., 2016).

Finally, Ψ_{MD} can be readily used as an irrigation scheduling threshold where limiting environmental factors are not a major concern (i.e. in arid regions where midday cloud cover is minimal). Therefore, for humid regions with intensive cloud cover, such as Georgia and much of the southeastern United States, Ψ_{MD} cannot be considered a valid reference for plant water status assessment (Chastain et al., 2016).

Predawn Leaf Water Potential

Predawn leaf water potential (Ψ_{PD}) indicates the maximum leaf water potential of a plant immediately before sunrise and can be used as an indicator of plant water status and for irrigation scheduling purposes (McMichael et al., 1973; Ameglio et al., 1999; Jones, 2004; Snider et al., 2014; Chastain, 2015; Chastain et al., 2016). Ψ_{PD} has been defined as less sensitive to environmental factors (VPD or cloud cover) than midday leaf water potential (Grimes et al., 1987),

and decreased water potential is associated with several physiological responses such as boll and leaf abscission for greenhouse-grown cotton (McMichael et al., 1987), leaf area, leaf size and plant height (Jordan et al., 1970; Turner et al, 1986) in cotton plants. In addition, Snider et al (2014) found a non-linear relationship between net photosynthesis (A_N) and Ψ_{PD} (Figure 1.3).

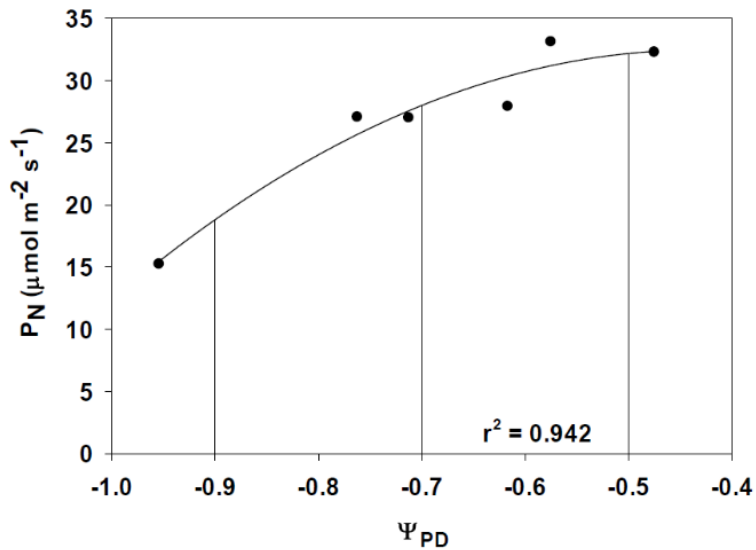


Figure 1.3 Relationship between Net Photosynthesis (A_N) and predawn leaf water potential (Ψ_{PD}), Snider et al. (2014).

Ψ_{PD} has successfully been used as an irrigation scheduling parameter in the Southeastern US (Chastain et al., 2016). However, the short time span when Ψ_{PD} data are collected limits the area a single individual could cover. Chastain et al. (2016) used Ψ_{PD} for irrigation scheduling by comparing dryland-grown and irrigated (using as irrigation thresholds Ψ_{PD} seasonal averages of -0.5MPa, -0.7MPa, -0.9MPa, and the checkbook method) cotton. Stable yields and a 7 to 31% decrease in water use were related to the different Ψ_{PD} treatments (Chastain et al., 2016). As a conclusion, predawn leaf water potential can be a reliable irrigation scheduling tool for areas where environmental factors limit the usefulness of Ψ_{MD} (Snider et al., 2015a).

Plant based methods-Indirect methods

Stem Diameter

Because cell expansion represents one of the most sensitive physiological processes to water deficit, plant parameters that are dependent on cell expansion can be sensitive indicators of water deficit (Hsiao, 1973). Among these indicators, stem diameter seems to be the most promising for scheduling irrigation (Jones, 2006; White and Raine, 2008; Snider et al., 2016). Stem diameter sensors can evaluate stem diameter variation as the plant grows (day-by-day change) or on a diurnal basis, to potentially estimate the quantity of water released through transpiration during the day or cell water content (Kozlowski, 1972; Garnier and Berger, 1986). Moreover, the evaluation of this swelling-shrinking process can be useful for scheduling irrigation by defining indices able to capture these variations. Unlike leaf water potential, stem diameter evaluation is a completely automated and non-destructive process (Fernandez and Cuevas, 2010).

Stem diameter variation (SDV) was the first indirect measure used to determine plant water status and to schedule irrigation (Hendrickson and Veihmeyer 1941; Molz and Klepper, 1973; Huguet et al., 1992; Cohen et al., 2001). However, SDV has been primarily used for tree species and very little for row crops (Vertessy et al., 1995; Wullschlegel and King, 2000; Olson and Rosell, 2013). Moreover, multi-day SDV data has been found to be extremely related to leaf water potential in corn and soybean (So et al., 1979).

In a literature review, Fernandez and Cuevas (2010) defined different indices much more sensitive to drought stress than leaf water potential or stomatal conductance; examples include stem growth rate (SGR) and maximum daily shrinkage (MDS). For cotton, MDS has been identified as a valid measure to schedule irrigation (Zhang et al., 2006; Flash, 2014). However, the most limiting factor when using these indices is the definition of reference diameter values for

non-water stressed plants among different growth stages, which could be a difficult task because of cultivar to cultivar variation (Gallardo et al., 2006a, b; Fernandez and Cuevas, 2010). Flash (2014) presented one of the most interesting applications of stem diameter sensors for scheduling irrigation in cotton. In fact, during the vegetative part of the growing season, stem diameter daily growth (in μm) has been correlated to SWT values at 30 cm, defining a recommended curve for optimal stem diameter daily growth (as shown in Figure 1.4).

Irrigation is triggered when the measured (actual) stem diameter daily growth curve goes below the recommended curve. Low stem diameter daily growth corresponds to increased SWT, indicating drought stress.

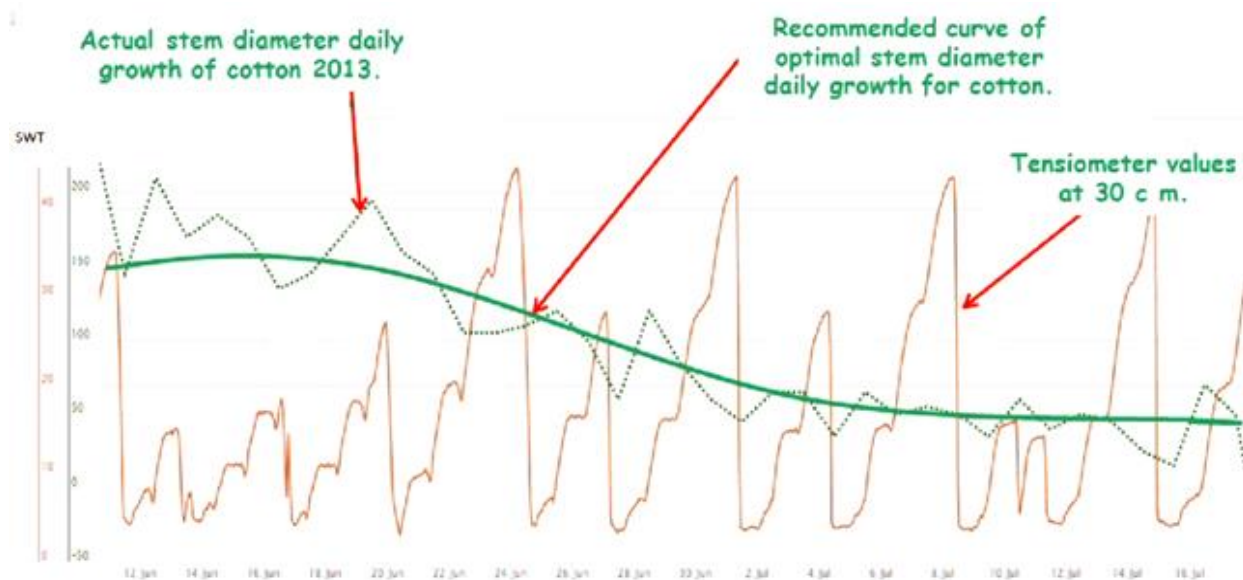


Figure 1.4 Stem diameter growth actual (dotted green line), recommended (continuous green line), and SWT curves (Flash, 2014)

For flowering and boll development, maximum daily stem contraction (or maximum daily shrinkage, MDS) was correlated to LWP (Flash, 2014). Following the same principle discussed

for stem daily growth, irrigation was triggered when the actual MDS curve exceeded the recommended curve, indicating SWT peaks (Figure 1.5).

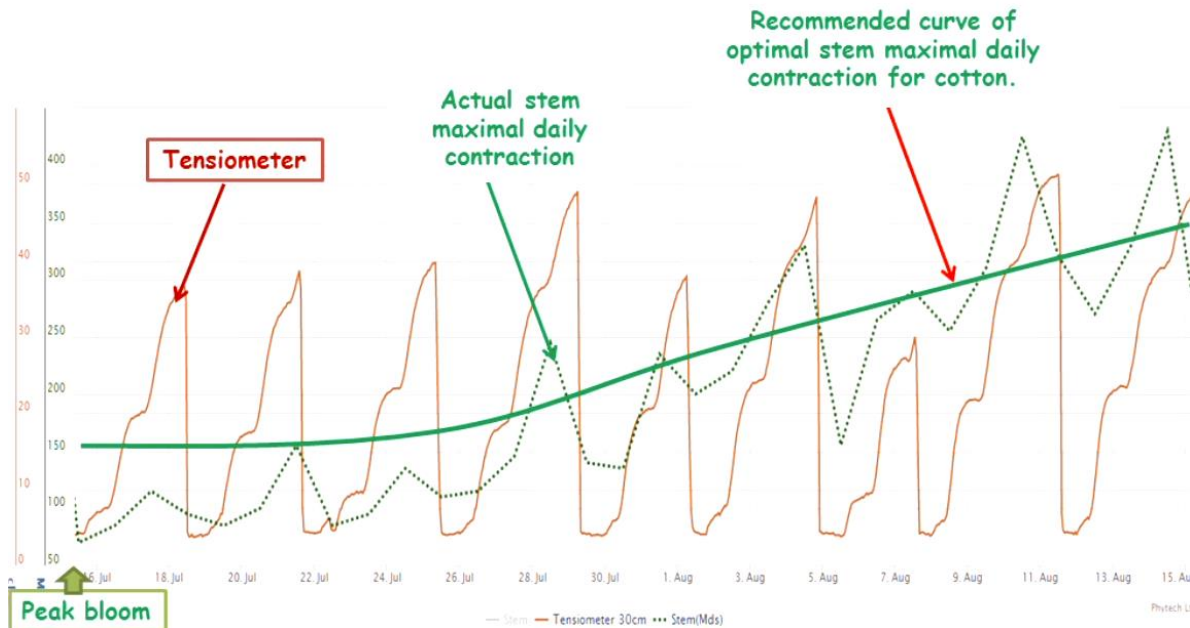


Figure 1.5 SWT, actual and recommended stem daily maximal contraction (Flash, 2014)

Infrared canopy temperature

Canopy temperature is another indirect plant-based approach to be used for scheduling irrigation (Jackson, 1981; Idso et al., 1981). Solar radiation is a fundamental aspect for plant photosynthesis, as previously discussed. Moreover, total absorbed radiation is dissipated in three primary ways: convection (heat dissipation with air movement), reradiation, and transpiration. For healthy plants with enough water available, transpiration represents the main mechanism for energy dissipation (Snider et al., 2015a). If the amount of energy dissipated is higher than the amount absorbed, leaf temperature will decrease, and vice versa (Hsiao, 1973; Taiz and Zeiger, 2010).

Canopy temperature has been defined as a strong indicator of plant water status (Gates 1964, Cohen et al., 2005). Over the years, several relationships between canopy temperature and other plant parameters have been investigated, including A_N , g_s , or LWP (Idso et al., 1981; Fuchs, 1990; Conaty et al., 2012; Snider et al., 2016). Ehrler (1973) used thermocouples embedded in cotton leaves to quantify canopy (T_c) – air temperature (T_a) changes. He found decreased T_c-T_a values after some hours from an irrigation event, and he also defined a linear relationship between leaf-air temperature difference and saturation deficit (SD), today referred as vapor pressure deficit (VPD; Jackson, 1981).

The stress-degree-day model where $SDD = T_c-T_a$, measuring both T_c and T_a 1.5 hours past solar noon, was defined by Idso et al (1977) and combined SDD with net radiation to predict ET, and thus crop water use. Successively, a normalized SDD-GDD (growing degree day) model, accounting for specific plant development differences, was presented by Idso et al. (1978). The SDD model considered canopy temperature higher than air temperature as an indicator of crop stress and a need for irrigation (Jackson, 1981). However, some later works (Idso et al., 1981) defined VPD as strongly able to influence this T_c-T_a differential, such that crop stress could occur even when T_c was below T_a . In addition, Idso et al (1982) defined several T_c-T_a to VPD non-water-stressed baselines for different crops.

The Crop Water Stress Index (CWSI) is one of the most widely known and used indices to evaluate crop water stress using canopy temperatures. It is defined as follows (Equation 8, Idso et al., 1981):

$$CWSI = \frac{T_{canopy} - T_{wet}}{T_{dry} - T_{wet}} \quad (8)$$

where T_{canopy} is the canopy temperature, T_{wet} is the temperature of a well-watered fully transpiring leaf, T_{dry} is the temperature of a completely non-transpiring leaf.

CWSI = 0 represents a healthy plant, CWSI = 1 represents a completely stressed plant (defined also as “non-transpiring” crop). Canopy temperatures can be defined by using thermometers, but also remote thermal images and values derived from satellites, hand-held devices, UAVs, or fixed field sensors (such as SmartCrop™; SmartField Inc, Lubbock, Texas; Porter et al., 2015). CWSI, as formulated and applied originally, had some limitations: (1) difficult separation of crop canopy temperatures from soil background (noise effect; Clarke, 1997); (2) difficult CWSI normalization under changing environmental conditions, such as cloud cover (Jones 1999; Jones et al., 2004). Canopy-related pixels can be separated in a thermal image from soil noise effect by defining upper and lower temperature limits, as in the following equation (Equation 9; Meron et al., 2010, 2013; Rud et al., 2014):

$$(T_{\text{air}} - 10) < T_{\text{cr}} < (T_{\text{air}} + 7) \tag{9}$$

where T_{air} is the air temperature, T_{cr} is the crop canopy temperature.

In addition to these factors, the recent use of remote sensing technologies brings different additional challenges, in particular the definition of an easy-to-use method to accurately extract canopy temperatures from large areas of a field captured using thermal imagery (Alchanatis et al., 2010). In fact, two main methods have been extensively used to calculate canopy temperature averages (Meron et al., 2010; Cohen et al., 2017):

Method 1. Considering the average of all the canopy pixels in the selected image/area.

$$T_{canopy} = \frac{\sum T_{cr_i} * f}{\sum f}$$

Method 2. Considering only the average temperature of the coldest 33 percent of the selected canopy pixels (Meron et al., 2010).

$$T_{canopy} = \frac{\sum_{i=1}^{0.33n} T_{cr_i} * f}{\sum_{i=1}^{0.33n} f_i}$$

where T_{canopy} is the canopy temperature, f is the frequency of points in each class (cr), n represents the total number of canopy related points.

Over the years, many different forms of empirical, theoretical, measured, or statistical dry and wet baselines have been defined in order to limit environmental variation when calculating CWSI and are summarized in the table below (Table 1.2; Cohen et al., 2017).

Empirical baselines. The empirical wet and dry baselines were firstly used by Idso et al. (1981). $T_c - T_a$ to VPD relationships were used to define upper ($T_c - T_a$ in severely stressed plants) and lower ($T_c - T_a$ in well-watered plants) baselines (Figure 1.6; Idso et al., 1981; Irmak et al., 2000). T_{dry} was estimated from the empirically derived well-watered baseline curve by using the linear equation to extend into the negative VPD axes by the temperature difference between canopy and air that exists at VPD = 0 (Idso et al., 1981; Jackson, 1991).

Table 1.2 Summary of wet and dry baseline types used for water status estimation (Cohen et al., 2017)

Baseline type		How is it calculated or measured?	Used for small scale	Used for large scale
Wet	Empirical	Air temperature + X °C where X is an empirical estimate dependent on VPD ^a	Irmak et al. (2000), Erdem et al. (2005), Jackson (1991), Shae et al. (1999)	Bellvert et al. (2014)
	Theoretical-1	Temperature calculation using energy balance equation (suggested by Jones 1992)	Jones (1999), Möller et al. (2007), Ben-Gal et al. (2009), Alchanatis et al. (2010)	
	Theoretical-2	Temperature calculation using energy balance equation (suggested by Monteith and Unsworth 1990)	Rud et al. (2014)	O'Shaughnessy et al. (2011)
	Measured: bio-indicator	Temperature measurement of a wet real leaf	Jones (1999)	
	Measured: artificial surface	Temperature measurement of a wet artificial reference surface	Cohen et al. (2005), Möller et al. (2007), Ben-Gal et al. (2009), Alchanatis et al. (2010), Meron et al. (2010)	
	Statistical/bio-indicator	Average temperature of the coolest 5–10% of the canopy pixels and the like	Alchanatis et al. (2010), Rud et al. (2014)	Gonzalez-Dugo (2013), Baluja et al. (2012)
Dry	Empirical	Air temperature + X °C where X is an empirical estimate ^a . The canopy-air temperature difference is unique for each crop in each region	Jackson (1991), Irmak et al. (2000), Cohen et al. (2005), Erdem et al. (2005), Möller et al. (2007), Alchanatis et al. (2010)	O'Shaughnessy et al. (2011), Gonzalez-Dugo et al. (2013), Meron et al. (2010)
	Theoretical	Temperature calculation using energy balance equations (suggested by Jones 1992)	Jones (1999), Möller et al. (2007), Ben-Gal et al. (2009)	
	Measured: bio indicator	Temperature measurement of a real leaf covered with petroleum jelly	Jones (1999)	

^a The canopy-air temperature difference is unique for each crop in each region and sometimes for each growth period

Some authors defined T_{dry} for cotton, grapevines, and olives as $T_{air} + 5\text{ }^{\circ}\text{C}$ (Irmak et al., 2000; Cohen et al., 2005; Alchanatis et al., 2010), and is today the most widely used method for T_{dry} or dry baseline calculation. In the same way, T_{wet} was defined as $T_{air} + X\text{ }^{\circ}\text{C}$, where X depends on leaf-air temperature differences to VPD for well-watered plants (lower baseline).

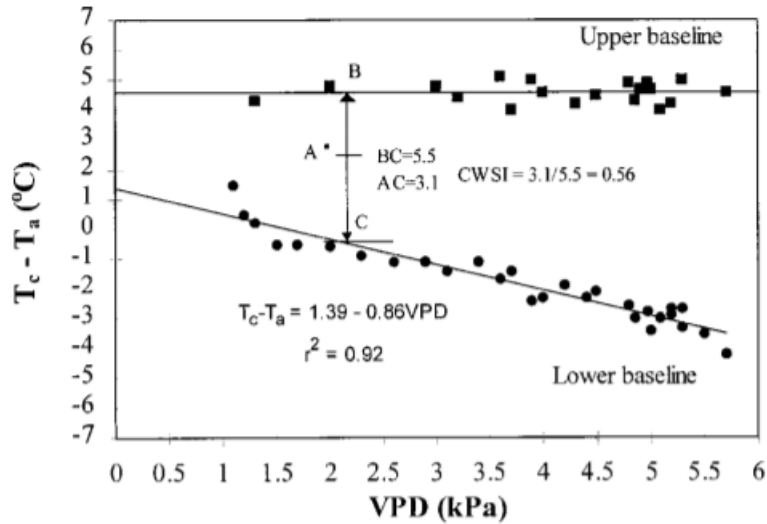


Figure 1.6 $T_c - T_a$ relationship with VPD for water-stressed and well-watered plants (Irmak et al., 2000).

Theoretical baselines. Theoretical wet and dry baselines can be calculated considering different energy balance equations (Monteith and Unsworth, 1990; Jones, 1999). The aim of these theoretical methods is limiting the baseline sensitivity to environmental variables, such as cloud cover and wind speed, by including them in the model. In particular, two main equations have been extensively used over the years for baseline calculations: the Jones (1999) leaf energy balance equation, and the energy balance equation suggested by Monteith and Unsworth (1990).

Theoretical 1 uses a model rearrangement of Jones (1999) Equation 9.6, to calculate T_{dry} and T_{wet} as follows (Equations 10; 11; 12; Jones, 1999; Möller et al., 2006; Alchanatis et al., 2010):

$$T_l - T_a = \frac{r_{HR}(r_{aW} + r_{lW})\gamma R_{ni}}{\rho c_p [\gamma(r_{aW} + r_{lW}) + s r_{HR}]} - \frac{r_{HR} \delta e}{\gamma(r_{aW} + r_{lW}) + s r_{HR}} \quad (10)$$

$$T_{dry} - T_a = \frac{r_{HR} R_{ni}}{\rho c_p} \quad (11)$$

$$T_{wet} - T_a = \frac{r_{HR} \delta e}{\gamma r_{aW} + s r_{HR}} \quad (12)$$

where $T_l - T_a$ is the leaf-air temperature difference, r_{HR} is the parallel resistance to heat and radiative transfer, r_{aW} is the boundary layer resistance to water vapor, r_{lW} is the leaf resistance to water vapour transfer (largely defined by stomatal resistance), γ is the psychrometric constant, R_{ni} is the net radiation that would be received by an equivalent surface at air temperature, ρ is the density of air, c_p is the specific heat capacity of air, s is the slope of the temperature to VPD curve, δe is air vapour pressure deficit.

Theoretical 2 uses the energy balance equation suggested by Monteith and Unsworth (1990) to define only T_{wet} , as shown in Equation 13 (O'Shaughnessy et al., 2012; Rud et al., 2014):

$$T_{wet} \approx T_a - \frac{e_s(T_a) - e_a}{\Delta + \gamma} \quad (13)$$

where T_a is the air temperature, e_s is the saturated vapor pressure deficit at T_a , e_a is the actual vapor pressure, Δ is slope of the temperature vs VPD curve, γ is the psychrometric constant.

Measured baselines: bio-indicator and artificial surface. Jones (1999) described a bio-indicator method to calculate both wet and dry baselines (Clawson et al., 1989; Jones, 1999). For T_{dry} calculation, both sides of the leaf were covered with petroleum jelly (Vaseline) in order to prevent transpiration. For T_{wet} , both sides of the leaf were wetted using a hand-held sprayer (water + detergent to increase adhesion). However, these real reference surfaces are difficult to maintain and can be evaluated only with hand-held devices and not with cameras or other automated systems due to possible shading effects.

Berliner et al. (1984) and Taghvaeian et al. (2014) have used reference well-watered plots to define a wet baseline but not for CWSI calculation (Cohen et al., 2017). However, this method requires to over irrigate a portion of the entire field, which usually does not represent the total variability among the entire area, to serve as a reference, but also overirrigated plants could have a different canopy growth pattern compared to plants under normal irrigation conditions (Alchanatis et al., 2010; Cohen et al., 2017). Furthermore, in large-scale producer fields, utilizing an over-irrigated, representative portion of the field to make irrigation scheduling decisions is impractical and at least partially negates the increase in water use efficiency that could be obtained through plant-based methods.

Another measured baseline type, used only for wet baseline calculation, is the so-called AWRS (artificial wet reference system) proposed by Meron et al. (2003). This AWRS consists of a polystyrene float covered by a wet non-woven viscose-polyester fabric in a double layer. The float is placed inside a 0.4 x 0.3 x 0.12 m constantly water-filled box (Cohen et al., 2005; Meron et al., 2010; Alchanatis et al., 2010) and connected to an IR thermal sensor mounted at 0.1 m above the reference surface. The whole system is placed together with a weather station (Meron et al., 2010). AWRS has been used for several studies in combination with empirical or theoretical dry

baselines to estimate CWSI (Cohen et al., 2005; Möller et al., 2006; Ben-Gal et al., 2009). This approach assumes that the evaporative cooling of the reference surface is comparable to that of a well-watered crop without constraints to transpiration (Meron et al., 2010).

Statistical baseline. Alchanatis et al. (2010) presented a statistical wet baseline calculated on the average temperature of the coolest 5% of the overall field canopy temperatures. This baseline was used for several studies, in combination with different dry baselines (Gonzalez-Dugo, 2013; Rud et al., 2014; Cohen et al., 2017).

Even though different studies have defined the empirical method ($T_{dry} = T_{air} + 5^{\circ}\text{C}$ in case of cotton, Irmak et al., 2000) as the best approach for T_{dry} estimation (Cohen et al., 2005; Alchanatis et al., 2010), different results have been reported when trying to identify the best approach for determining a wet baseline (Jones et al., 2002; Alchanatis et al., 2010; Baluja et al., 2012; Cohen et al., 2017). Moreover, most of the studies compared only two baseline approaches, or evaluated the applicability of these baselines on a small-scale (Jones et al., 2002; Baluja et al., 2012). Jones et al. (2002) conducted a detailed study, considering different wet and dry baselines for CWSI calculation in vineyards.

In a successive study on drip-irrigated cotton, Chastain et al. (2016) used SmartCrop TM (SmartField, Lubbock, TX) infrared thermometers to evaluate T_{canopy} averages from 1200 to 1400 h for irrigation purposes during 2013 and 2014 growing seasons. Empirical wet and dry baselines ($T_{air} + X^{\circ}\text{C}$) were defined (Idso, 1981). CWSI was calculated using a rearranged Eq. 1 (Equation 14), as follows:

$$CWSI = \frac{[(T_{canopy} - T_{air}) - (T_{NWS} - T_{air})]}{[(T_{dry} - T_{air}) - (T_{NWS} - T_{air})]} \quad (14)$$

CWSI values were calculated and coupled with Ψ_{PD} during the whole irrigation period (starting at cotton squaring) for two years. This was the first documentation of a very strong relationship ($R^2 = 0.93$, Figure 1.7) between CWSI and Ψ_{PD} in the Southeastern US, and in the State of Georgia, where environmental aspects strongly limit the usefulness of LWP readings (Chastain et al., 2013; 2016). CWSI plot values over the growing seasons 2013 and 2014 were also related to lint yield (Figure 1.7).

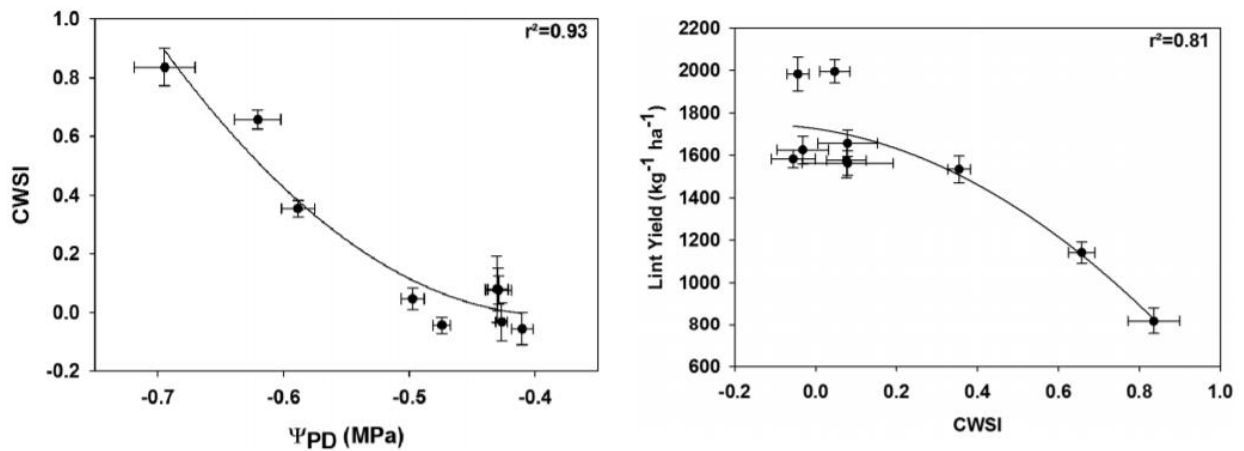


Figure 1.7 CWSI and Ψ_{PD} relationship (on the left); CWSI and Lint Yield relationship (on the right; Chastain et al., 2016)

The latest and most exhaustive comparison study on different baselines used for water status mapping in Israel was presented by Cohen et al. (2017). In this study, empirical, theoretical, measured, and statistical wet baselines and different T_{canopy} were investigated to define the best baseline combination. All the different approaches were evaluated considering the correlations between measured LWPs and calculated LWPs, but also the applicability of each approach as a farmer-friendly tool. T_{dry} was calculated as $T_{\text{air}} + 5 \text{ }^\circ\text{C}$ in all the CWSI combinations. For T_{canopy} , the two different scenarios were (1) considering 100% of canopy values, or (2) considering only the coldest 33% of canopy values. Several well-watered baselines (T_{wet}) were calculated: (i) empirical wet baseline, using $T_c - T_a$ differences to VPD; (ii) two theoretical wet baselines, one

using Jones energy balance equation (1999), the other using Penman and Monteith energy balance equation (1990); (iii) bio-indicator wet baseline, measuring temperature of a wet real leaf; (iv) ARWS wet baseline, measuring the temperature of a wet reference surface; (v) statistical wet baseline, averaging the 5% of the coolest canopy pixels (Cohen et al., 2017). CWSI was calculated using Equation 1. CWSI maps for all the different methods were converted into LWP maps, using the following formula (Cohen et al., 2015; Equation 15):

$$LWP [MPa] = -1.77CWSI - 1.28 - K \quad (15)$$

where K is the transformation constant (for K an empirical value of 0.4 MPa was used).

CWSI-derived LWP maps were successively compared to measured LWP values (Cohen et al., 2017). As a result, the best two regression models were found to be (i) T_{canopy} calculated as the coldest 33% of the whole canopy pixels and T_{wet} defined using the energy balance equation suggested by Monteith and Unsworth (1990), (ii) T_{canopy} calculated as the coldest 33% of the whole canopy pixels and T_{wet} calculated considering the coldest 5% of the total canopy pixel values.

In addition, LWP maps were divided into pre-determined classes in order to categorize water status (Table 1.3; Cohen et al., 2005; Alchanatis et al., 2010; Cohen et al., 2017).

Table 1.3 Defined classes for water status mapping (Cohen et al., 2017)

Class	Water status description	LWP range (MPa)
1	Over-irrigated (Oir)	$[-1.45] \geq LWP > [\text{RecLWP} + \text{RMSE}]$
2	Well irrigated (WI)	$[\text{RecLWP} + \text{RMSE}] \geq LWP > [\text{RecLWP} - \text{RMSE}]$
3—20—50 DAF ^a	Low water stress (LWS)	$[\text{RecLWP} - \text{RMSE}] \geq LWP > [-2.4]$
3—50—70 DAF	Low water stress (LWS)	$[\text{RecLWP} - \text{RMSE}] \geq LWP > [-3.0]$
4—20—50 DAF	Medium to sever water stress (MSWS)	$[-2.4] \geq LWP$
4—50—70 DAF	Medium to sever water stress (MSWS)	$[-3.0] \geq LWP$

^a Days after flowering onset

While most of the previous studies were focused on the definition of small-scale application methods (Cohen et al., 2005; Alchanatis et al., 2010; Meron et al., 2010; Rud et al., 2014), the innovative concept of this study is the definition of a scientifically-valid approach for large-scale applications. Moreover, the creation of CWSI-to-LWP maps could be used to better define a “farmer-friendly” automated tool for irrigation purposes (Vellidis et al., 2014; Cohen et al., 2017).

In a similar manner, a comparable approach could be implemented for areas strongly affected by environmental factors, such as Southeastern US. Direct measures of plant water status and physiological response to irrigation could be investigated to define possible relationships with CWSI using the aforementioned approaches (Chastain et al., 2016).

RATIONALE

Direct and indirect estimates of crop water status and need for irrigation have been widely used for irrigation scheduling purposes. ET-based water balance irrigation scheduling approaches as the UGA Checkbook method were shown to increase irrigation use efficiency (IWUE) when compared to conventional irrigation scheduling based on visual signs of crop status. In addition, soil moisture sensors have also been used to trigger irrigation, improving yields and irrigation use efficiency (Vellidis et al., 2016). In the humid Southeastern US, SmartCrop™-based Crop Water Stress Index (CWSI) has been successfully associated with water-induced yield variability and physiological parameters, such as predawn leaf water potential (Ψ_{PD}).

Novel thermal imaging systems, providing near-continuous canopy temperature data throughout the season, have tremendous potential to be coupled with variable rate irrigation. Specifically, capturing crop water status in real time would allow the definition of irrigation management zones (IMZs) as the crop develops, and the appropriate irrigation amounts could be supplied only when and where the crop needs it. Given the limited amount of information available on the use of these innovative thermal systems, validation with well-established indicators of crop water status is essential.

The objectives of the current study were: (1) validate a novel thermal camera system, using well-established crop water status sensing methods and (2) calculate the previously discussed CWSIs from camera-derived canopy temperatures and relate them to established IRT-based CWSIs and crop physiological responses.

References:

- Ackerson, R. C., & Hebert, R. R. (1981). Osmoregulation in cotton in response to water stress: I. Alterations in photosynthesis, leaf conductance, translocation, and ultrastructure. *Plant physiology*, 67(3), 484-488.
- Ackerson, R. C., Krieg, D. R., Haring, C. L., & Chang, N. (1977). Effects of Plant Water Status on Stomatal Activity, Photosynthesis, and Nitrate Reductase Activity of Field Grown Cotton 1. *Crop Science*, 17(1), 81-84.
- Alchanatis, V., Cohen, Y., Cohen, S., Moller, M., Sprinstin, M., Meron, M., ... & Sela, E. (2010). Evaluation of different approaches for estimating and mapping crop water status in cotton with thermal imaging. *Precision Agriculture*, 11(1), 27-41.
- Allen, R. G., Pereira, L. S., Raes, D., & Smith, M. (1998). Crop evapotranspiration-Guidelines for computing crop water requirements-FAO Irrigation and drainage paper 56. Fao, Rome, 300(9), D05109.
- Améglio, T., Archer, P., Cohen, M., Valancogne, C., Daudet, F. A., Dayau, S., & Cruiziat, P. (1999). Significance and limits in the use of predawn leaf water potential for tree irrigation. *Plant and Soil*, 207(2), 155-167.
- Baluja, J., Diago, M. P., Balda, P., Zorer, R., Meggio, F., Morales, F., & Tardaguila, J. (2012). Assessment of vineyard water status variability by thermal and multispectral imagery using an unmanned aerial vehicle (UAV). *Irrigation Science*, 30(6), 511-522.
- Ben-Gal, A., Agam, N., Alchanatis, V., Cohen, Y., Yermiyahu, U., Zipori, I., ... & Dag, A. (2009). Evaluating water stress in irrigated olives: correlation of soil water status, tree water status, and thermal imagery. *Irrigation Science*, 27(5), 367-376.
- Berliner, P., Oosterhuis, D. M., & Green, G. C. (1984). Evaluation of the infrared thermometer as a crop stress detector. *Agricultural and Forest meteorology*, 31(3-4), 219-230.
- Bolger, T. P., Upchurch, D. R., & McMichael, B. L. (1992). Temperature effects on cotton root hydraulic conductance. *Environmental and Experimental Botany*, 32(1), 49-54.
- Carmo-Silva, A. E., Gore, M. A., Andrade-Sanchez, P., French, A. N., Hunsaker, D. J., & Salvucci, M. E. (2012). Decreased CO₂ availability and inactivation of Rubisco limit photosynthesis in cotton plants under heat and drought stress in the field. *Environmental and Experimental Botany*, 83, 1-11.
- Chastain, D. R. (2015). Defining drought sensitivity and assessing alternative irrigation practices for *Gossypium hirsutum* grown in the southeastern United States. PhD diss. Athens, GA: University of Georgia, Department of Crop and Soil Sciences.

- Chastain, D. R., Snider, J. L., Collins, G. D., Perry, C. D., Whitaker, J., & Byrd, S. A. (2014). Water deficit in field-grown *Gossypium hirsutum* primarily limits net photosynthesis by decreasing stomatal conductance, increasing photorespiration, and increasing the ratio of dark respiration to gross photosynthesis. *Journal of Plant Physiology*, 171(17), 1576-1585.
- Chastain, D. R., Snider, J. L., Collins, G. D., Perry, C. D., Whitaker, J., Byrd, S. A., ... & Porter, W. M. (2016). Irrigation scheduling using predawn leaf water potential improves water productivity in drip-irrigated cotton. *Crop Science*, 56(6), 3185-3195.
- Chastain, D. R., Snider, J. L., Collins, G. D., Whitaker, J., & Perry, C. D. (2013). Plant Water Status and Leaf Temperature as Indicators of Water Deficit Stress in Cotton. *Research and Extension Report 2012*, 56.
- Clarke, T. R. (1997). An empirical approach for detecting crop water stress using multispectral airborne sensors. *HortTechnology*, 7(1), 9-16.
- Clawson, K. L., Jackson, R. D., & Pinter, P. J. (1989). Evaluating plant water stress with canopy temperature differences. *Agronomy Journal*, 81(6), 858-863.
- Cohen, M., Goldhamer, D. A., Fereres, E., Girona, J., & Mata, M. (2001). Assessment of peach tree responses to irrigation water deficits by continuous monitoring of trunk diameter changes. *The Journal of Horticultural Science and Biotechnology*, 76(1), 55-60.
- Cohen, Y., Alchanatis, V., Meron, M., Saranga, Y., & Tsipris, J. (2005). Estimation of leaf water potential by thermal imagery and spatial analysis. *Journal of experimental botany*, 56(417), 1843-1852.
- Cohen, Y., Alchanatis, V., Saranga, Y., Rosenberg, O., Sela, E., & Bosak, A. (2017). Mapping water status based on aerial thermal imagery: comparison of methodologies for upscaling from a single leaf to commercial fields. *Precision Agriculture*, 18(5), 801-822.
- Cohen, Y., Alchanatis, V., Sela, E., Saranga, Y., Cohen, S., Meron, M., Bosak, A., Tsipris, J., Ostrovsky, V., Orolov, V., & Levi, A. (2015). Crop water status estimation using thermography: Multi-year model development using ground-based thermal images. *Precision Agriculture*, 16(3), 311-329.
- Conaty, W. C., Burke, J. J., Mahan, J. R., Neilsen, J. E., & Sutton, B. G. (2012). Determining the optimum plant temperature of cotton physiology and yield to improve plant-based irrigation scheduling. *Crop Science*, 52(4), 1828-1836.
- Conaty, W. C., Mahan, J. R., Neilsen, J. E., & Constable, G. A. (2014). Vapour pressure deficit aids the interpretation of cotton canopy temperature response to water deficit. *Functional plant biology*, 41(5), 535-546.

Cornic, G., & Fresneau, C. (2002). Photosynthetic carbon reduction and carbon oxidation cycles are the main electron sinks for photosystem II activity during a mild drought. *Annals of Botany*, 89(7), 887-894.

Cutler, J., & Rains, D. W. (1977). Effects of Irrigation History on Responses of Cotton to Subsequent Water Stress 1. *Crop science*, 17(2), 329-335.

Dang, Q. L., Margolis, H. A., Coyea, M. R., Sy, M., & Collatz, G. J. (1997). Regulation of branch-level gas exchange of boreal trees: roles of shoot water potential and vapor pressure difference. *Tree Physiology*, 17(8-9), 521-535.

Davidson Jr, J. I., Lamb, M. C., & Sternitzke, D. A. (2000). Farm suite-Irrigator Pro (Peanut irrigation software, and user's guide). The Peanut Foundation, Alexandria, VA.

Davies, W. J., & Zhang, J. (1991). Root signals and the regulation of growth and development of plants in drying soil. *Annual review of plant biology*, 42(1), 55-76.

Day, M. E. (2000). Influence of temperature and leaf-to-air vapor pressure deficit on net photosynthesis and stomatal conductance in red spruce (*Picea rubens*). *Tree Physiology*, 20(1), 57-63.

Díaz, M. B., Zunzunegui, M., Esquivias, M. P., Boutaleb, S., Valera-Burgos, J., Tagma, T., & Ain-Lhout, F. (2013). Some secrets of *Argania spinosa* water economy in a semiarid climate. *Natural product communications*, 8(1), 11-14.

Ehrler, W. L. (1973). Cotton Leaf Temperatures as Related to Soil Water Depletion and Meteorological Factors 1. *Agronomy Journal*, 65(3), 404-409.

Ennahli, S., & Earl, H. J. (2005). Physiological limitations to photosynthetic carbon assimilation in cotton under water stress. *Crop Science*, 45(6), 2374-2382.

Fernández, J. E., & Cuevas, M. V. (2010). Irrigation scheduling from stem diameter variations: a review. *Agricultural and Forest Meteorology*, 150(2), 135-151.

Fisher, K., & Udeigwe, T. (2012). Cotton water requirements. *Cotton Irrigation Management for Humid Regions*. Cary, NC: Cotton Incorporated, 14-16.

Flash, I. (2014). Can plant-based moisture sensing improve irrigation scheduling and water use efficiency? Practical cotton remote sensing project, Israel 2013. In *Proceedings of the 2014 Beltwide Cotton Conferences (USA)*.

Flexas, J., & Medrano, H. (2002). Drought-inhibition of photosynthesis in C3 plants: stomatal and non-stomatal limitations revisited. *Annals of botany*, 89(2), 183-189.

Flexas, J., Escalona, J. M., & Medrano, H. (1999). Water stress induces different levels of photosynthesis and electron transport rate regulation in grapevines. *Plant, Cell & Environment*, 22(1), 39-48.

Flexas, J., Galmes, J., Ribas-Carbo, M., & Medrano, H. (2005). The effects of water stress on plant respiration. In *Plant respiration* (pp. 85-94). Springer, Dordrecht.

Forti, R., & Henrard, M. (2016) Eurostat, Agriculture, forestry, and fishery statistics 2016 edition. Eurostat. Retrieved from <https://ec.europa.eu/eurostat/documents/3217494/7777899/KS-FK-16-001-EN-N.pdf/cae3c56f-53e2-404a-9e9e-fb5f57ab49e3>

Fuchs, M. (1990). Infrared measurement of canopy temperature and detection of plant water stress. *Theoretical and Applied Climatology*, 42(4), 253-261.

Gallardo, M., Thompson, R. B., Valdez, L. C., & Fernández, M. D. (2006a). Response of stem diameter variations to water stress in greenhouse-grown vegetable crops. *The Journal of Horticultural Science and Biotechnology*, 81(3), 483-495.

Gallardo, M., Thompson, R. B., Valdez, L. C., & Fernández, M. D. (2006b). Use of stem diameter variations to detect plant water stress in tomato. *Irrigation Science*, 24(4), 241-255.

Garnier, E., & Berger, A. (1986). Effect of water stress on stem diameter changes of peach trees growing in the field. *Journal of Applied Ecology*, 193-209.

Gates, D. M. (1964). Leaf Temperature and Transpiration 1. *Agronomy Journal*, 56(3), 273-277.

Gonzalez-Dugo, V., Zarco-Tejada, P., Nicolás, E., Nortes, P. A., Alarcón, J. J., Intrigliolo, D. S., & Fereres, E. (2013). Using high resolution UAV thermal imagery to assess the variability in the water status of five fruit tree species within a commercial orchard. *Precision Agriculture*, 14(6), 660-678.

Grimes, D. W., & Yamada, H. (1982). Relation of Cotton Growth and Yield to Minimum Leaf Water Potential 1. *Crop Science*, 22(1), 134-139.

Grimes, D. W., Yamada, H., & Hughes, S. W. (1987). Climate-normalized cotton leaf water potentials for irrigation scheduling. *Agricultural Water Management*, 12(4), 293-304.

Hendrickson, A. H., & Veihmeyer, F. J. (1941). Moisture distribution in soil in containers. *Plant physiology*, 16(4), 821.

Hsiao, T. C. (1973). Plant responses to water stress. *Annual review of plant physiology*, 24(1), 519-570.

Huguet, J. G., Li, S. H., Lorendeau, J. Y., & Pelloux, G. (1992). Specific micromorphometric reactions of fruit trees to water stress and irrigation scheduling automation. *Journal of Horticultural Science*, 67(5), 631-640.

Idso, S. B. (1982). Non-water-stressed baselines: a key to measuring and interpreting plant water stress. *Agricultural Meteorology*, 27(1-2), 59-70.

Idso, S. B., Jackson, R. D., & Reginato, R. J. (1977). Remote-sensing of crop yields. *Science*, 196(4285), 19-25.

Idso, S. B., Jackson, R. D., & Reginato, R. J. (1978). Extending the "degree day" concept of plant phenological development to include water stress effects. *Ecology*, 59(3), 431-433.

Idso, S. B., Jackson, R. D., Pinter Jr, P. J., Reginato, R. J., & Hatfield, J. L. (1981). Normalizing the stress-degree-day parameter for environmental variability. *Agricultural Meteorology*, 24, 45-55.

Irmak, S., Haman, D. Z., & Bastug, R. (2000). Determination of crop water stress index for irrigation timing and yield estimation of corn. *Agronomy Journal*, 92(6), 1221-1227.

Jackson, R. D., Idso, S. B., Reginato, R. J., & Pinter Jr, P. J. (1981). Canopy temperature as a crop water stress indicator. *Water resources research*, 17(4), 1133-1138.

Jackson, S. H. (1991). Relationships between normalized leaf water potential and crop water stress index values for acala cotton. *Agricultural Water Management*, 20(2), 109-118.

Jones, H. G. (1973). Moderate-term water stresses and associated changes in some photosynthetic parameters in cotton. *New Phytologist*, 72(5), 1095-1105.

Jones, H. G. (1999). Use of infrared thermometry for estimation of stomatal conductance as a possible aid to irrigation scheduling. *Agricultural and forest meteorology*, 95(3), 139-149.

Jones, H. G. (2004). Irrigation scheduling: advantages and pitfalls of plant-based methods. *Journal of experimental botany*, 55(407), 2427-2436.

Jones, H. G. (2006). Monitoring plant and soil water status: established and novel methods revisited and their relevance to studies of drought tolerance. *Journal of experimental botany*, 58(2), 119-130.

Jones, H. G., Stoll, M., Santos, T., Sousa, C. D., Chaves, M. M., & Grant, O. M. (2002). Use of infrared thermography for monitoring stomatal closure in the field: application to grapevine. *Journal of Experimental Botany*, 53(378), 2249-2260.

Jordan, W. R. (1970). Growth of Cotton Seedlings in Relation to Maximum Daily Plant-Water Potential 1. *Agronomy journal*, 62(6), 699-701.

- Kisekka, I., Migliaccio, K. W., Dukes, M. D., Schaffer, B., & Crane, J. H. (2010). Evapotranspiration-based irrigation scheduling and physiological response in a carambola (*Averrhoa Carambola* L.) orchard. *Applied engineering in agriculture*, 26(3), 373-380.
- Kitao, M., & Lei, T. T. (2007). Circumvention of over-excitation of PSII by maintaining electron transport rate in leaves of four cotton genotypes developed under long-term drought. *Plant Biology*, 9(1), 69-76.
- Kozlowski, T. T. (1972). Shrinking and swelling of plant tissues. *Water deficits and plant growth*, 3, 1-64.
- Krieg, D. R., & Sung, J. F. M. (1986). Source-sink relations as affected by water stress during boll development. *Cotton physiology*, 7377.
- Lacape, M. J., Wery, J., & Annerose, D. J. M. (1998). Relationships between plant and soil water status in five field-grown cotton (*Gossypium hirsutum* L.) cultivars. *Field Crops Research*, 57(1), 29-43.
- Lawlor, D. W., & Tezara, W. (2009). Causes of decreased photosynthetic rate and metabolic capacity in water-deficient leaf cells: a critical evaluation of mechanisms and integration of processes. *Annals of botany*, 103(4), 561-579.
- Liakos, V., Vellidis, G., Tucker, M., Lowrance, C., & Liang, X. (2015). A decision support tool for managing precision irrigation with center pivots. In *Precision agriculture'15* (pp. 713-720). Wageningen Academic Publishers.
- Liang, X., Liakos, V., Wendroth, O., & Vellidis, G. (2016). Scheduling irrigation using an approach based on the van Genuchten model. *Agricultural Water Management*, 176, 170-179.
- Liu, R. X., Zhou, Z. G., Guo, W. Q., Chen, B. L., & Oosterhuis, D. M. (2008). Effects of N fertilization on root development and activity of water-stressed cotton (*Gossypium hirsutum* L.) plants. *Agricultural water management*, 95(11), 1261-1270.
- Loka, D. A., & Oosterhuis, D. M. (2012). Water stress and reproductive development in cotton. *Flowering and Fruiting in Cotton*. Cordova: The Cotton Foundation, 51-58.
- Loka, D. A., Oosterhuis, D. M., & Ritchie, G. L. (2011). Water-deficit stress in cotton. *Stress physiology in cotton*, 7, 37-72.
- Long, S. P., & Bernacchi, C. J. (2003). Gas exchange measurements, what can they tell us about the underlying limitations to photosynthesis? Procedures and sources of error. *Journal of experimental botany*, 54(392), 2393-2401.
- Massacci, A., Nabiev, S. M., Pietrosanti, L., Nematov, S. K., Chernikova, T. N., Thor, K., & Leipner, J. (2008). Response of the photosynthetic apparatus of cotton (*Gossypium hirsutum*)

to the onset of drought stress under field conditions studied by gas-exchange analysis and chlorophyll fluorescence imaging. *Plant physiology and biochemistry*, 46(2), 189-195.

McMichael, B. L., Jordan, W. R., & Powell, R. D. (1973). Abscission Processes in Cotton: Induction by Plant Water Deficit 1. *Agronomy Journal*, 65(2), 202-204.

McMichael, B. L., Oosterhuis, D. M., Zak, J. C., & Beyrouthy, C. A. (2010). Growth and development of root systems. In *Physiology of cotton* (pp. 57-71). Springer, Dordrecht.

McMichael, B. L., Quisenberry, J. E., & Upchurch, D. R. (1987). Lateral root development in exotic cottons. *Environmental and experimental botany*, 27(4), 499-502.

Medrano, H., Escalona, J. M., Bota, J., Gulías, J., & Flexas, J. (2002). Regulation of photosynthesis of C3 plants in response to progressive drought: stomatal conductance as a reference parameter. *Annals of botany*, 89(7), 895-905.

Meron, M., Sprintsin, M., Tsipris, J., Alchanatis, V., & Cohen, Y. (2013). Foliage temperature extraction from thermal imagery for crop water stress determination. *Precision Agriculture*, 14(5), 467-477.

Meron, M., Tsipris, J., & Charitt, D. (2003). Remote mapping of crop water status to assess spatial variability of crop stress. In *Precision agriculture. Proceedings of the fourth European conference on precision agriculture*. Academic Publishers, Berlin (pp. 405-410).

Meron, M., Tsipris, J., Orlov, V., Alchanatis, V., & Cohen, Y. (2010). Crop water stress mapping for site-specific irrigation by thermal imagery and artificial reference surfaces. *Precision agriculture*, 11(2), 148-162.

Migliaccio, K. W., Morgan, K. T., Vellidis, G., Zotarelli, L., Fraise, C., Zurweller, B. A., ... & Rowland, D. L. (2016). Smartphone apps for irrigation scheduling. *Transactions of the ASABE*, 59(1), 291-301.

Migliaccio, K.W., Debastiani Andreis, J.H., Fraise, C., Morgan, K.T., and Vellidis, G. (2013). Smartirrigation apps: urban turf. AE499 Agricultural and Biological Engineering Department, Florida Cooperative Extension Service, Institute of Food and Agricultural Sciences, University of Florida. Retrieved from <http://edis.ifas.ufl.edu/ae499>

Möller, M., Alchanatis, V., Cohen, Y., Meron, M., Tsipris, J., Naor, A., ... & Cohen, S. (2006). Use of thermal and visible imagery for estimating crop water status of irrigated grapevine. *Journal of experimental botany*, 58(4), 827-838.

Molz, F. J., & Klepper, B. (1973). On the Mechanism of Water-Stress-Induced Stem Deformation 1. *Agronomy Journal*, 65(2), 304-306.

Monteith, J. L., & Unsworth, M. H. (1990). *Principles of environmental physics*. London: Edward Arnold. Olson, M. E., & Rosell, J. A. (2013).

Vessel diameter–stem diameter scaling across woody angiosperms and the ecological causes of xylem vessel diameter variation. *New Phytologist*, 197(4), 1204-1213.

Oosterhuis, D. M. (1981). Hydraulic conductivity and drought acclimation of cotton root systems. Ph.D. diss. Logan, Utah: Utah State University.

Oosterhuis, D. M., & Wullschleger, S. D. (1987a). Osmotic adjustment in cotton (*Gossypium hirsutum* L.) leaves and roots in response to water stress. *Plant Physiology*, 84(4), 1154-1157.

Oosterhuis, D. M., & Wullschleger, S. D. (1987b). Water flow through cotton roots in relation to xylem anatomy. *Journal of experimental botany*, 38(11), 1866-1874.

Oosterhuis, D. M., & Wullschleger, S. D. (1988). Carbon partitioning and photosynthetic efficiency during boll development. In *Proceedings-Beltwide Cotton Production Research Conferences (USA)*.

O'Shaughnessy, S. A., Evett, S. R., Colaizzi, P. D., & Howell, T. A. (2012). A crop water stress index and time threshold for automatic irrigation scheduling of grain sorghum. *Agricultural water management*, 107, 122-132.

Pallas, J. E., Michel, B. E., & Harris, D. G. (1967). Photosynthesis, transpiration, leaf temperature, and stomatal activity of cotton plants under varying water potentials. *Plant Physiology*, 42(1), 76-88.

Perry, C. D., Barnes, E. M., Munk, D., Fisher, K., & Bauer, P. (2012). Cotton irrigation management for humid regions. Cotton Incorporated.

Perry, S. W., Krieg, D. R., & Hutmacher, R. B. (1983). Photosynthetic rate control in cotton: Photorespiration. *Plant Physiology*, 73(3), 662-665.

Pettigrew, W. T. (2004). Physiological consequences of moisture deficit stress in cotton. *Crop Science*, 44(4), 1265-1272.

Porter, W. M., Snider, J. L., Perry, C. D., Monfort, W. S., & Vellidis, G. (2015). SmartCrop® Sensors for Predicting Irrigation Requirements for Peanut in the Southeast. In *2015 ASABE Annual International Meeting* (p. 1). American Society of Agricultural and Biological Engineers.

Rosenthal, W. D., Arkin, G. F., Shouse, P. E., & Jordan, W. R. (1987). Water Deficit Effects on Transpiration and Leaf Growth 1. *Agronomy Journal*, 79(6), 1019-1026.

Rud, R., Cohen, Y., Alchanatis, V., Levi, A., Brikman, R., Shenderoy, C., ... & Mulla, D. (2014). Crop water stress index derived from multi-year ground and aerial thermal images as an indicator of potato water status. *Precision agriculture*, 15(3), 273-289.

Sanders, G. J., & Arndt, S. K. (2012). Osmotic adjustment under drought conditions. In *Plant Responses to Drought Stress* (pp. 199-229). Springer, Berlin, Heidelberg.

Sharp, R. E., Poroyko, V., Hejlek, L. G., Spollen, W. G., Springer, G. K., Bohnert, H. J., & Nguyen, H. T. (2004). Root growth maintenance during water deficits: physiology to functional genomics. *Journal of experimental botany*, 55(407), 2343-2351.

Shock, C. C., Akin, A., Unlenen, L., Feibert, E. G. B., Nelson, K., & Tschida, A. (2003). A comparison of soil water potential and soil water content sensors. *Special Report*, 1048, 235-240.

Shock, C. C., Barnum, J. M., & Seddigh, M. (1998). *Calibration of Watermark Soil Moisture Sensors for Irrigation Management*.

Snider, J. L., Chastain, D. R., Meeks, C. D., Collins, G. D., Sorensen, R. B., Byrd, S. A., & Perry, C. D. (2015b). Predawn respiration rates during flowering are highly predictive of yield response in *Gossypium hirsutum* when yield variability is water-induced. *Journal of plant physiology*, 183, 114-120.

Snider, J. L., Collins, G. D., Whitaker, J., Perry, C. D., & Chastain, D. R. (2014). Electron transport through photosystem II is not limited by a wide range of water deficit conditions in field-grown *Gossypium hirsutum*. *Journal of Agronomy and Crop Science*, 200(1), 77-82.

Snider, J. L., Collins, G. D., Whitaker, J., Perry, C. D., & Chastain, D. R. (2013) The effect of water deficit on photosynthetic electron transport and net CO₂ assimilation rates in field-grown cotton. *Georgia Cotton Research and Extension Report*, 51–55.

Snider, J.L. & Oosterhuis D. M. (2015a). *Physiology. Cotton 2nd edition* (pp 339-400). D. Fang and R. Percy. Madison, WI. ASA-CSSA-SSSA.

Snider, J.L. and Chastain D.R. (2016) *Plant-Based Irrigation Scheduling. Linking Physiology to Management* (pp 97-116). Snider J.L. and Oosterhuis D.M. The Cotton Foundation, Cordova, TN.

So, H. B., Reicosky, D. C., & Taylor, H. M. (1979). Utility of Stem Diameter Changes as Predictors of Plant Canopy Water Potential 1. *Agronomy Journal*, 71(5), 707-713.

Taghvaeian, S., Comas, L., DeJonge, K. C., & Trout, T. J. (2014). Conventional and simplified canopy temperature indices predict water stress in sunflower. *Agricultural water management*, 144, 69-80.

Taiz, L., & Zeiger, E. (2010). *Plant physiology 5th Ed.* Sunderland, MA: Sinauer Associates.

Taylor, H. M., & Klepper, B. (1979). The Role of Rooting Characteristics in the Supply of Water to Plants 1. In *Advances in agronomy* (Vol. 30, pp. 99-128). Academic Press.

- Tezara, W., Mitchell, V. J., Driscoll, S. D., & Lawlor, D. W. (1999). Water stress inhibits plant photosynthesis by decreasing coupling factor and ATP. *Nature*, 401(6756), 914.
- Thomson, S. J., & Armstrong, C. F. (1987). Calibration of the Watermark model 200 soil moisture sensor. *Applied Engineering in Agriculture*, 3(2), 186-189.
- Turner, N. C., Hearn, A. B., Begg, J. E., & Constable, G. A. (1986). Cotton (*Gossypium hirsutum* L.): Physiological and morphological responses to water deficits and their relationship to yield. *Field Crops Research*, 14, 153-170.
- Turner, N. C., Stern, W. R., & Evans, P. (1987). Water Relations and Osmotic Adjustment of Leaves and Roots of Lupins in Response to Water Deficits 1. *Crop Science*, 27(5), 977-983.
- USDA National Agricultural Statistics Service. (2014). Farm and Ranch Irrigation Survey 2013. Retrieved from https://www.nass.usda.gov/Publications/AgCensus/2012/Online_Resources/Farm_and_Ranch_Irrigation_Survey/fris13.pdf
- Van Genuchten, M. T. (1980). A closed-form equation for predicting the hydraulic conductivity of unsaturated soils 1. *Soil science society of America journal*, 44(5), 892-898.
- Vellidis, G., Liakos, V., Perry, C., Tucker, M., Collins, G., Snider, J., Andreis, J., Migliaccio, K., Fraise, C., Morgan, K. and Rowland, D. (2014). A smartphone app for scheduling irrigation on cotton. In *Proceedings of the 2014 Beltwide Cotton Conference*, New Orleans, LA, National Cotton Council, Memphis, TN.
- Vellidis, G., Liakos, V., Porter, W., Tucker, M., & Liang, X. (2016). *A Dynamic Variable Rate Irrigation Control System*. St. Louis, Missouri: Academic Publishers.
- Vellidis, G., Tucker, M., Perry, C., Kvien, C., & Bednarz, C. (2008). A real-time wireless smart sensor array for scheduling irrigation. *Computers and electronics in agriculture*, 61(1), 44-50.
- Vellidis, G., Tucker, M., Perry, C., Reckford, D., Butts, C., Henry, H., Liakos, V., Hill, R.W. and Edwards, W. (2013). A soil moisture sensor-based variable rate irrigation scheduling system. In *Precision agriculture'13* (pp. 713-720). Wageningen Academic Publishers, Wageningen.
- Vertessy, R. A., Benyon, R. G., O'sullivan, S. K., & Gribben, P. R. (1995). Relationships between stem diameter, sapwood area, leaf area and transpiration in a young mountain ash forest. *Tree physiology*, 15(9), 559-567.
- Vories, E. D., Teague, T., Greene, J., Stewart, J., Clawson, E., Pringle, L., & Phipps, B. (2006). Determining the optimum timing for the final irrigation on mid-South cotton. In *Proceedings National Cotton Council Beltwide Cotton Conference* (pp. 516-521).

Whitaker, J., Culpepper, S., Freeman, M., Harris, G., Kemerait, B., Perry, C., Porter, W., Roberts, P., Shurley, D., Smith, A. (2018). Georgia Cotton Production Guide. Cooperative Extension, University of Georgia.

White, S. C., & Raine, S. R. (2008). A grower guide to plant based sensing for irrigation scheduling. National Centre for Engineering in Agriculture, University of Southern Queensland.

White, S. C., & Raine, S. R. (2009). Physiological response of cotton to a root zone soil moisture gradient: implications for Partial Root Zone Drying irrigation. *Journal of Cotton Science*, 13(2), 67-74.

Wullschleger, S. D., & King, A. W. (2000). Radial variation in sap velocity as a function of stem diameter and sapwood thickness in yellow-poplar trees. *Tree Physiology*, 20(8), 511-518.

Zhang, J. Y., Duan, A. W., Meng, Z. J., & Liu, Z. G. (2006). Suitability of stem diameter variations as an indicator of water stress of cotton. *Agricultural Sciences in China*, 5(5), 356-362.

Zhang, Y. L., Hu, Y. Y., Luo, H. H., Chow, W. S., & Zhang, W. F. (2011). Two distinct strategies of cotton and soybean differing in leaf movement to perform photosynthesis under drought in the field. *Functional Plant Biology*, 38(7), 567-575.

Zotarelli, L., Dukes, M. D., Romero, C. C., Migliaccio, K. W., & Morgan, K. T. (2010). Step by step calculation of the Penman-Monteith Evapotranspiration (FAO-56 Method). Institute of Food and Agricultural Sciences. University of Florida.

CHAPTER 2

VALIDATION OF A NOVEL THERMAL IMAGING SYSTEM FOR COTTON IRRIGATION SCHEDULING IN THE SOUTHEASTERN USA

Abstract

Thermal imagery of crop canopy has shown to be an accurate indicator of crop water status and successfully deployed as an irrigation scheduling tool for cotton.

The objective of the current study was to validate a novel camera approach to other systems known for accurately represent crop water status, as IRTs and soil moisture sensors. To this end, a study was conducted consisting of a split plot randomized complete block design with three cultivars and 3 different irrigation treatments: Dryland, 100% of crop evapotranspiration (ET_C) supplied (well-watered), and 125% of ET_C (overirrigated). Crop water status (predawn water potential, midday water potential, and midday stomatal conductance) and crop response measurements (growth and physiology) were collected for each plot every week (when possible), beginning at cotton squaring. Several CWSIs were derived from thermal images and IRTs and relationships defined with the aforementioned plant parameters.

Physiological (predawn and midday leaf water potential, stomatal conductance) and growth parameters showed no cultivar, irrigation or irrigation x cultivar treatment effect due to the enormous amount of rainfall observed during the growing season. The novel imaging system showed to agree with SmartCrop™ IRT ($r^2 = 0.842$) and soil moisture-based ($r^2 = 0.585$) methods indicating the system could be used to accurately estimate crop water status and as an irrigation scheduling tool.

Keywords: variable rate irrigation, soil moisture sensor, thermal imagery, irrigation management zones, crop water stress index, pre-dawn leaf water potential.

Introduction:

Drought stress is a major constraint to crop productivity (Hsiao et al., 1973). Water deficit affects cotton (*Gossypium hirsutum* L.) development to different extents based on the intensity, the duration of the stress event, and the growth stage when the stress occurs (Snider et al., 2015). Root elongation in cotton has been shown to be less sensitive to water stress than shoot elongation (Sharp et al., 2004). Relative differences in osmotic adjustment, greater in roots than in leaves, explains the lower water sensitivity of cotton roots to water stress. Water stress also decreases the total leaf area available for photosynthesis and the average photosynthetic efficiency of all leaves in the canopy, which negatively impacts fruit retention (Krieg and Sung, 1986). For cotton, Oosterhuis and Wullschleger (1988) defined a strong relationship between the size of fully matured sympodial leaves [cm^2] and the respective weights [g] of the bolls they subtend. This suggests a drought stress-induced leaf area decrease could impact boll size. Although flowers are protected from drought stress and abscission, small cotton floral buds are extremely sensitive to drought stress (Loka and Oosterhuis, 2012). Also, small bolls are the most sensitive to stress. In fact, even though drought can negatively impact boll mass, a greater percentage of dry weight is distributed to the lint, which offsets boll size effects. Therefore, boll density per hectare is the main limitation to lint yield under drought (Hu et al. 2018). In addition, lint yield has been shown to be more impacted from water stress than fiber quality (Pettigrew, 2004).

Efficient irrigation scheduling methods are important to increase economic productivity in today's agriculture. Farmers are commonly basing their irrigation decisions on visual signs of drought stress such as wilting (USDA, 2013 Farm and Ranch Irrigation Survey; Snider et al., 2016). However, these irrigation practices usually lead to penalized yields, representing inefficient irrigation scheduling approaches. Vories et al. (2006) estimated incorrect irrigation timing in

cotton can result in yield losses between 150-750 \$/acre. In recent years, improvements in irrigation scheduling approaches have been used to achieve higher yields and better irrigation water use efficiency (IWUE). The University of Georgia Checkbook method (Whitaker et al., 2018) is a long-tested and widely-disseminated scheduling method, where irrigation is used as a supplement to rainfall in order to reach weekly targets. This method represents an easy-to-use tool for farmers and has been shown to increase yields and WUE, when compared to conventional irrigation scheduling based on water balance methods; however, advanced environmental approaches and plant-based irrigation scheduling can greatly increase WUE over the checkbook approach (Vellidis et al., 2016). For example, the Smart Irrigation Cotton App (Vellidis et al., 2014) is an advanced water balance method where climatic data (evapotranspiration, precipitation, etc) are included in calculations of crop water use. However, water balance methods do not consider the possible differences in soil type or moisture over a large field, and a flat irrigation rate is applied to all these different areas. The University of Georgia Smart Sensor Array (UGA SSA) soil moisture sensing system is one method available to address this limitation. Soil moisture values are collected and coupled with soil water retention curves to calculate zone-specific irrigation recommendations, allowing variable rate irrigation (VRI). Soil moisture sensor approaches have been well-documented to generate the highest yields and greatest water savings among all the aforementioned indirect methods (Vellidis et al., 2016).

While these methods are valuable irrigation scheduling tools, they do not provide information on plant water status. This is important because the plant integrates its total environment and interacts with it in a dynamic manner. For example, plant factors such as rooting depth and leaf area development are responsive to environmental conditions and can influence soil water availability and rate of use by the crop. For these reasons, irrigation should be triggered

based on plant-based measures of crop water status. Stem diameter is one of the earliest plant-based parameters investigated for irrigation scheduling applications (Molz and Klepper, 1973). Recently, Flash (2014) correlated soil water tension measurements to cotton stem daily growth during the vegetative part of the growing season, and to maximum stem daily contraction (MDS) between flowering and boll development. Leaf water potential, both predawn (Ψ_{PD}) and midday (Ψ_{MD}), has been the most investigated direct, plant-based method for irrigation scheduling. In many cases it is used as a validation tool for indirect plant-based parameters such as thermal imagery (Cohen et al., 2005; Ben-Gal et al., 2009). Thermal imagery of the crop canopy has been widely used for detecting plant stress (Jones et al., 1999, 2002; Chastain et al., 2016). Plants tend to close stomata during a drought stress period to limit the amount of water lost, increasing leaf temperature (Hsiao, 1973). The Crop Water Stress Index (CWSI; Idso et al., 1981) exploits this mechanism. In Israel, a specific relationship between midday leaf water potential and Crop Water Stress Index has been defined and used to generate leaf water potential maps from thermal camera-based canopy temperatures. This is important information for cotton producers in Israel since drip irrigation scheduling in cotton is managed according to stage-specific leaf water potential thresholds (Alchanatis et al., 2010; Cohen et al., 2005, 2017). In the humid Southeastern US, where environmental variability and cloud cover limit the usefulness of midday leaf water potential measurements, predawn leaf water potential, shown to be less sensitive to environmental changes, has been strongly related to infrared thermometer-based Crop Water Stress Index, and a season-long Ψ_{PD} irrigation threshold of -0.5 MPa was recommended for maximizing water use efficiency in drip-irrigated cotton (Chastain et al., 2016).

However, infrared thermometers and most thermal cameras mounted to ground or air-based platforms lack the ability to cover extensive agricultural areas with high frequency data collection.

Thus, short-lived environmental fluctuations can play an important role in limiting the quality of data collected (Jones et al., 1999). Using novel thermal imaging systems able to collect near-continuous canopy temperatures on a large scale would allow for the definition of canopy temperature-based transient irrigation management zones throughout the season, and to define specific irrigation thresholds in real-time. Being able to accurately estimate crop water status and simultaneously apply irrigation only when the crop needs it and in the proper amounts, would increase crop yields at the field level while also decreasing water use. Because information is limited on these new thermal imaging systems, validation by means of well-established sensing methods is a fundamental step toward defining whether these systems are capable of accurately representing canopy temperature and crop water status.

The objectives of the current study were: (1) validate a novel thermal camera system, using well-established crop water status sensing methods and (2) calculate the previously discussed CWSIs from camera-derived canopy temperatures and relate them to established IRT-based CWSIs and crop physiological responses.

Materials and Methods

Site description and Plant material

To validate the use of a novel, canopy sensing system as valid indicator of crop water status, research plots were established on approximately 1.03 hectare at C.M. Stripling Irrigation Research Park near Camilla, GA (31° 16' 55.2"N, 84° 17' 38.04"W) during the 2018 growing season. Prior to planting, Telone II (Dow AgroSciences LLC, IN) soil fumigant was applied via a KMC (Kelley Manufacturing Co., Tifton, GA) strip-till implement. The implement tilled the rows to a depth of approximately 0.30 m. On May 2, 2018 cotton (*Gossypium hirsutum* L.) seeds from

three different varieties, shown to differ in the response of stomatal conductance to VPD (PHY 330 – PhytoGen, Dow AgroSciences LLC, IN; PHY 490 – PhytoGen, Dow AgroSciences LLC, IN; ST 6182 GLT – Bayer - Stoneville Cotton; Dr. Avat Shekoofa, personal communication), were planted at a 2.5cm (1-inch) depth, 0.91m inter-row spacing, and seeding rate of 10 seeds m⁻¹. Buffer zones between the irrigation zones (discussed in more detail below) were planted using PHY 440 (PhytoGen, Dow AgroSciences LLC, IN) seeds. Each plot was 4 rows wide and 12.2 m in length. Plots were separated East-West by variable-row buffers and North-South by 14.6 m alleys, to ensure a proper transition of the irrigation system, when changing rates from one plot to the other.

Irrigation Treatments and Sampling Procedures

Irrigation was managed according to three different irrigation treatments, using a modified University of Georgia Smart Irrigation Cotton App calculation spreadsheet: Rainfed (no irrigation), 100% ET method - considering 100% of daily ET_C for deficit calculations (well-watered), and 125% ET method - considering 125% of daily ET_C for deficit calculations (over-irrigated). Daily deficit was calculated as the simple difference between crop evapotranspiration (ET_C = K_C *ET₀) and irrigation (I) + precipitation (P). ET₀ was defined using the FAO 56 Penman-Monteith equation (Allen et al., 1998). A linear-move, variable rate, sprinkler irrigation system (Valley Irrigation, Valley, NE, USA) was used to supply the different irrigation rates. Irrigation was triggered, based on root zone soil water deficit (RZSWD) values from the modified Cotton App spreadsheet, when RZSWD exceeded 50% deficit before flowering, and 15% deficit after flowering (Vellidis et al., 2014). When the irrigation threshold was exceeded, irrigation was applied to fill the soil profile and go back to 0% deficit when possible. To avoid runoff and nutrient

or pesticide leaching the maximum irrigation rate was set at 2 cm (0.8 in) per application. For irrigation, an application efficiency factor of 0.85 was applied, for precipitation the efficiency factor was 0.9. The 15% deficit threshold during flowering was used to accommodate our irrigation system limitations while still applying the ET requirements of each irrigation treatment. The plots were irrigated on May 3, 2018 to ensure adequate soil moisture for germination. Thereafter, the aforementioned irrigation treatments were imposed. For season-total irrigation amounts and number of irrigation events for each treatment see Table 2.1

Fertilization and pest management were conducted according to the University of Georgia Cooperative Extension's 2018 Cotton Production Guide (Whitaker et al., 2018). All the physiological measurements (predawn and midday leaf water potential (Ψ_{PD} , Ψ_{MD}), gas exchange measurements, in-season plant growth and light interception) were collected on a weekly basis (when possible), starting at the onset of cotton squaring (when floral buds were first visible). Weather data were provided by the Georgia Automated Environmental Monitoring Network (GAEMN, <http://www.weather.uga.edu/>) weather station located at the Stripling Irrigation Research Park in Camilla, GA near our experimental field of interest (31° 16' 48.29" N, -84° 17' 29.8" W). The soil type in the study area was a lucy loamy sand (loamy, kaolinitic) with 0 to 5 percent slopes (NRCS – web soil survey).

Soil moisture assessments

To monitor soil moisture condition, 27 University of Georgia Smart Sensor Array (UGA SSA) sensors were installed in the experimental plots on May 23, 2018. 1 node per plot was installed in all the ST 6182 GLT plots for a total number of 18. The remaining 9 nodes were split

between the other two cultivars, considering all the possible cv x irrigation combinations. Each installed node was composed of three integrated Watermark ® soil moisture sensors (Irrometer, Riverside, California, USA) placed at three different depths, for cotton at 0.15, 0.30, and 0.45 m below the soil surface. Data from each single moisture sensor was sent to the base station using a “mesh” network (where the signal moves from one node to another to finally reach the base station). The base station, located at the border of the experimental area, was responsible for uploading the data to the web server. Finally, weighted soil water tension (the absolute value of soil matric potential) averages of the three moisture sensors were calculated and displayed on the dedicated website (<https://ugassa.flintirrigation.com/>) every day at 0700 h. Two different weighted averages were displayed on the website: (1) Shallow weighted average, calculated as $0.6 * \text{soil water tension at 15cm} + 0.4 * \text{soil water tension at 30cm}$; (2) Deep weighted average, calculated as $0.5 * \text{soil water tension at 15cm} + 0.3 * \text{soil water tension at 30cm} + 0.2 * \text{soil water tension at 45cm}$. For cotton, the deep weighted average was considered a better indicator of soil “dryness” and crop stress (Vellidis et al., 2016).

Canopy temperature and CWSI acquisition and validation

Canopy temperature (T_c) was measured using two different systems: (1) SmartCrop™-infrared thermometers, and the (2) Sentinel™- thermal camera (SmartField, Lubbock, TX). The SmartCrop™ (SmartField, Lubbock, TX) infrared system uses a ZyTemp (ZyTemp, HsinChu, Taiwan) TN901 Infrared module with a measurement range of -33 to 220 °C and ± 3 °C in accuracy. For this project, 27 SmartCrops™ were installed on June 13th, 2018 in the same plots where soil moisture sensors were already present. SmartCrop™ sensors were adjusted in height during the season to maintain them 30 cm above the canopy and at a 60° angle with respect to the

horizontal plane. The sensors recorded temperature values every minute and generated 15-minute averages. Data was sent from each individual sensor to the base station using a wireless network. Temperature values were collected during the irrigation period and filtered to include only canopy averages between 1200 and 1400 h, on days where solar radiation was greater than 600 W m^{-2} (Chastain et al., 2016). Canopy temperatures were not collected on fertilizer, growth regulator or pesticide application dates.

In addition to the SmartCrop™ infrared thermometers, a 360° rotating thermal infrared camera (Sentinel™) was placed on the east edge of the experimental area. The camera was mounted on an extendable pole and lifted to a final height of 15 meters (48 ft). The pole was leveled and anchored to the ground using a large tripod structure along with stakes and guy wires to maintain stability. The Sentinel™ camera was oriented towards the plots after the installation. Several images were taken on an hourly basis. The resulting radiometric data collected were processed and stitched directly from SmartField™, and the final panorama view of the area was displayed on their website (<http://fit2.smartfield.com>). In addition to the panorama, valuable as a display tool but not for data analysis, temperature averages were calculated for each individual plot, considering all the pixels within the plot itself. Plots were drawn using an open source, Java-based image processing software called ImageJ. Plots were defined for each one of the 9 individual images used in the image stitching process. For plots present in different individual images, all the temperature values were averaged to estimate the final plot temperature average. Canopy temperature, air temperature, and relative humidity averages were generated for each plot every 15 minutes and downloaded as comma separated file spreadsheet. For data analysis, canopy temperature averages were calculated during the irrigation period and filtered to include only canopy averages between 1200 and 1400 h, on days where solar radiation was greater than 600 W

m⁻². Plot-average canopy temperatures were used for calculating different Crop Water Stress Indices (CWSI; Idso et al., 1981; Monteith and Unsworth, 1990; Jones, 1999): (1) Idso CWSI, following the formula and baselines defined in Idso et al. (1981); (2) Jones1 CWSI, calculated using the energy balance approach described in Jones (1999) for both dry and wet baselines; (3) Jones2 CWSI, calculated using air temperature + 5°C as dry baseline and the Jones (1999) energy balance equation as wet baseline; Monteith CWSI, calculated using air temperature + 5°C as dry baseline and the Monteith and Unsworth (1990) energy balance equation as wet baseline. All four different Crop Water Stress Indices were calculated for both SmartCrop™-derived and Sentinel™-derived temperature averages. Weather data used for energy balance calculations were retrieved from the GAEMN's weather station located at the Stripling Irrigation Research Park in Camilla, GA. Air temperature from the SmartCrop™ base station was used for calculating both Sentinel™-based and SmartCrop™-based CWSIs (Chastain et al., 2016).

For the Idso et al. (1981) Crop Water Stress Index Calculation, well-watered baselines were generated for both SmartCrops™ and the Sentinel™ thermal camera, by averaging canopy temperature for the 125% ET treatment plots (over-irrigated treatment) from 1200 to 1400h, between June 26th and July 26th, 2018, on days where solar radiation was greater than 600 W m⁻² (Chastain et al., 2016). Canopy-air temperature differences were then plotted against air vapor pressure deficit (VPD) and the relationship T_c-T_a vs VPD (well-watered baseline) was estimated using linear regression for both SmartCrop™ and Sentinel™ temperature data. For the empirical CWSI (Idso), dry baseline was estimated using the methodology described by Idso et al. (1981), by extending the well-watered baseline into the negative VPD region the same magnitude as the leaf-air VPD that exists when air VPD = 0. CWSI values were calculated according to the following equation: $CWSI = [(T_C - T_{air}) - (T_{wet} - T_{air})] / [(T_{dry} - T_{air}) - (T_{wet} - T_{air})]$, where CWSI

= 0 represents a healthy and fully transpiring plant, and CWSI = 1 a completely non-transpiring crop (Idso et al., 1981). The generated SmartCrop™-based well-watered baseline and Idso CWSI values were compared to the previously defined Chastain et al. (2016) baseline and CWSI. SmartCrop™-derived Idso CWSI values for all the different irrigation treatments and sampling dates were also plotted against the Sentinel™-derived Idso CWSI values calculated on all the different sampling dates to investigate a possible relationship.

Midday and Predawn leaf water potential

In the study, the different Crop Water Stress Indices were coupled with predawn (Ψ_{PD}) and midday (Ψ_{MD}) leaf water potential estimates. Ψ_{PD} was measured between 0400 and 0600 h and Ψ_{MD} between 1200 and 1400 h, once per week (when possible) beginning at cotton squaring. Ψ_{PD} and Ψ_{MD} were measured using a Scholander pressure chamber (615 Model, PMS Instruments, Albany, OR). The pressure chamber was cleaned, repaired, and recalibrated by the manufacturer before the beginning of the growing season. A single leaf per plot was excised and the petiole of the excised leaf was immediately sealed using a rubber gasket, in order to maintain the excised surface (petiole) exposed to the air. The leaf blade was sealed and inserted into the chamber and the chamber was pressurized at a rate of 0.05 to 0.1 MPa s⁻¹. Between leaf excision and the beginning of chamber pressurization 5-10 s elapsed. Pressurization ended when water first appeared at the cut surface of the petiole and a plot Ψ_{PD} or Ψ_{MD} value was recorded. Measurements were conducted on the uppermost fully-expanded leaf (fourth leaf node below the plant terminal). Predawn and midday leaf water potentials were collected on June 07th, June 15th, June 21st, July 5th, July 12th, July 27th, August 8th, and August 23rd, 2018.

Gas exchange measurements

In addition to predawn and midday leaf water potentials, midday single-leaf gas exchange measurements were collected on the same sampling dates noted above from 1200 to 1400 h, using an LI-6800 (LI-COR Biosciences, Lincoln, NE) portable photosynthesis system. Gas exchange parameters (stomatal conductance to water vapor (g_s), net photosynthesis (A_n), and leaf to air VPD), leaf temperature, and chamber air temperature were collected for each plot. The specific warm-up tests and calibration procedures were performed right before each sampling time. Chamber temperature and relative humidity (RH) were set to mimic ambient temperature and humidity at the time of measurement. All the measurements were conducted on the uppermost fully expanded leaf using a light intensity of $1500 \mu\text{mol m}^{-2} \text{s}^{-1}$ photosynthetically active radiation (PAR), above the light saturation point for net photosynthesis in cotton (Constable and Oosterhuis, 2010). Intrinsic water use efficiency (iWUE; $\mu\text{mol CO}_2 \text{ mol}^{-1}\text{H}_2\text{O}$) was then calculated for each plot as: $\text{iWUE} = A_n/g_s$.

In-season plant growth and light interception

Cotton growth parameters (number of mainstem nodes and plant height) and light interception were collected as well on the same previously discussed sampling dates. Number of mainstem nodes and plant height were measured on five plants per plot. The five measurements were averaged to define a representative value for each plot prior to statistical analysis. Photosynthetically active radiation (PAR) was collected using an AccuPAR LP-80 (Decagon Devices Inc., Pullman, WA) ceptometer. PAR readings were taken below the canopy, using the 19 x 9.5 mm cross-section, 84 cm probe incorporated with AccuPAR LP-80 and above the canopy,

using an external PAR sensor mounted on a tripod 1.5 m above the surface and connected to the ceptometer. Two different above and below-canopy PAR measurements (1- placing the AccuPAR probe in the row middles (parallel to the cotton rows); 2- placing the AccuPAR probe perpendicularly across a cotton row) were taken simultaneously on days with low cloud cover and within ± 1.5 h from solar noon (Earl and Davis, 2003). The two different measurements per plot were averaged to get a unique PAR above and PAR below value.

In addition, canopy interception of photosynthetically active radiation (IPAR) was calculated as:

$$IPAR = 1 - \left(\frac{\text{average PAR below}}{\text{average PAR above}} \right)$$

Immediately before cotton defoliation (~60% open boll), IPAR was evaluated one final time as previously described and all plants present in a 1-meter section of each plot were destructively harvested and dried at 80°C in a forced-air oven for 60 h to determine total above-ground dry weight (DW) in g m^{-2} . Cumulative total solar radiation data from planting until harvest (MJ m^{-2}) at the Camilla site was obtained from the aforementioned weather station on-site. Total solar radiation was converted to photosynthetically active radiation by assuming that PAR represents 45% of total solar radiation (Monteith, 1965; Meek et al., 1984; Kiniry et al., 1989). Total IPAR for the growing season ($IPAR_{\text{total}}$; MJ m^{-2}) was quantified by multiplying whole-season, plot-average IPAR by cumulative PAR. Radiation use efficiency (RUE) for each plot was quantified by dividing crop DW in g m^{-2} by IPAR total in MJ m^{-2} . Thus, cumulative above-ground DW, $IPAR_{\text{total}}$, and RUE for each irrigation treatment are provided in Table 2.2.

Statistical Methods

The experimental design of the study was a split-plot complete randomized block design with three cultivars, three irrigation treatments, and six replications where irrigation was the main plot factor and cultivar the sub-plot factor. The effects of irrigation, cultivar, and the interaction term irrigation x cultivar were evaluated using a mixed-effect, two-way analysis of variance (ANOVA). Blocks were treated as a random effect, whereas irrigation treatment and cultivar were considered fixed effects. Post hoc analysis was conducted using Fisher's protected LSD. Data analysis was conducted using JMP Pro 13 (SAS Institute, Cary, NC) and graphs drawn using SigmaPlot 14 (Systat Software Inc). For Ψ_{PD} , Ψ_{MD} , mainstem height and nodes, IPAR, A_n , g_s , intrinsic WUE, leaf T, leaf-air T, leaf-air VPD graphs each data point represents the average of 18 data points for every sampling date. For well-watered baseline determination (Figure 2.7 a, b), canopy-air temperature averages of 18 replicate plots for Sentinel™ and 9 replicate plots for SmartCrop™ (the total number of plots in the 125% ET treatment) were plotted versus VPD on the dates noted previously in this report. The Idso, Jones1, Jones2, and Monteith CWSIs were calculated for all the different sampling dates as the average of 54 (for Sentinel™-derived CWSIs) or 27 data points (for SmartCrop™-derived CWSIs). Linear regression was used to determine the relationships between Sentinel™-derived and SmartCrop™-derived CWSI, Root Zone Soil Water Deficit, and for both Sentinel™ and SmartCrop™-based well-watered baselines because it provided a better fit than the second-order, polynomial model. Moreover, all the CWSI to CWSI or CWSI to RZSWD relationships were found to be significant ($P < 0.05$). For all the other parameters (Ψ_{PD} , Ψ_{MD} , mainstem height and nodes, IPAR, A_n , g_s , intrinsic WUE, leaf T, leaf-air T, leaf-air VPD, DW, $IPAR_{total}$, average IPAR and RUE), no significant cultivar, irrigation or

cultivar by irrigation interaction effects were observed ($P > 0.05$). Therefore, data were averaged by irrigation treatment on all the different sampling dates for graphic visualization only.

Results and Discussion

Air Temperature, Rainfall, and Root Zone Soil Water Deficit

Daily maximum and minimum air temperature, and rainfall amounts throughout the 2018 growing season, from planting to defoliation, from the GAEMN weather station located in Camilla, GA are shown in Figure 2.1. During the 2018 season total rainfall from planting to defoliation was 80.68 cm, while cotton only needs around 46 cm of rainfall to optimize yields in Georgia (Bednarz et al., 2002). Rainfall was equally distributed during the growing season, and water deficit rarely occurred. Soil water tension data, as well as root zone soil water deficit (RZSWD) for the rainfed treatment, highlight how moderate to high water stress was verified only at the end of June, with a maximum RZSWD value of 35.4% (corresponding to an average deep SWT value of 63.53 kPa) on June 24th, and in the middle of July, with maximum RZSWD of 51.9% (deep SWT of 38.94 kPa) on July 18th. Deep soil water tension values collected during the whole growing season agreed with root zone soil water deficit as shown in Figure 2.2 for the 100% ET irrigation treatment. As previously documented, the relationship between SWT and RZSWD strongly depends on soil type and should be adjusted considering the characteristics of the investigated area (Vellidis et al., 2016). In our case, the suggested Cotton App thresholds of 70kPa (or 50% RZSWD) before flowering and 40kPa (or 50% RZSWD) after the beginning of flowering seem to reflect appropriate water stress levels to be used for cotton irrigation scheduling.

Predawn and Midday Leaf Water Potential and Growth Parameters

The constant well-watered condition of the experimental area, due to the large amount of rainfall during the growing season, is shown for each sampling date in Figure 2.3 a, b. Ψ_{PD} ranged from a minimum of -0.45 MPa (on the third sampling date - June 21st) to a maximum of -0.2 MPa (on the first sampling date - June 7th). Ψ_{MD} ranged from a maximum of -0.8MPa on July 27th to a minimum around -1.3MPa on June 21st. Therefore, Ψ_{PD} and Ψ_{MD} values have been sensibly higher than values indicated to sensibly impact metabolic function or cotton yields (Loka and Oosterhuis, 2012; Chastain et al., 2016).

Considering cotton growth parameters, mainstem height (Figure 2.4a) started around 40 cm at the beginning of squaring (37.4 cm for Rainfed; 36.3 cm for 100% ET treatment; 36.9 cm for 125% ET treatment) and stabilized between 120-140 cm at first open boll (122.4 cm for Rainfed; 135.8 cm for 100% ET treatment; 130.5 cm for 125% ET treatment). Mainstem nodes (Figure 2.4b) for the different irrigation treatments ranged from 7 nodes/plant at the beginning of squaring to almost 19 nodes/plant (18.3 nodes/plant for Rainfed; 18.7 nodes/plant for 100% ET treatment; 18.4 nodes/plant for 125% ET treatment) at first open boll stage. In addition, canopy interception of photosynthetically active radiation (IPAR; Figure 2.4c) showed a typical sigmoidal shaped curve (Earl and Davis, 2003; Oosterhuis and Wullschleger, 1988), with a “plateau” effect at 0.9-0.95 (90-95%) canopy interception.

Single leaf Gas Exchange Parameters and Intrinsic WUE

A_n and g_s showed a similar trend during the 2018 growing season (Figure 2.5a, b), with a constant slow increase until reaching a peak on July 27th (for A_n : 42.6 $\mu\text{mol m}^{-2} \text{s}^{-1}$ for Rainfed;

39.4 $\mu\text{mol m}^{-2} \text{s}^{-1}$ for 100% ET treatment; 39.8 $\mu\text{mol m}^{-2} \text{s}^{-1}$ for 125% ET treatment; and for g_s : 1.78 $\text{mol m}^{-2} \text{s}^{-1}$ for Rainfed; 1.76 $\text{mol m}^{-2} \text{s}^{-1}$ for 100% ET treatment; 1.79 $\text{mol m}^{-2} \text{s}^{-1}$ for 125% ET treatment), and after that a decrease. Intrinsic WUE (iWUE), calculated as A_n/g_s (Figure 2.5c), started at 60-70 $\mu\text{mol CO}_2 \text{ mol}^{-1}\text{H}_2\text{O}$ and constantly decreased as the season progressed, stabilizing around 22-27 $\mu\text{mol CO}_2 \text{ mol}^{-1}\text{H}_2\text{O}$ after the beginning of July. The high A_n and g_s values were comparable to previous observations with well-watered, field-grown cotton, indicating limited to no water stress occurred during the growing season (Baker et al., 2007; Chastain et al., 2014).

LI-6800 Leaf Temperature, Leaf-Air, and Leaf to Air VPD

Leaf temperature started low ($\sim 29\text{-}30$ °C) and sharply increased and stabilized at 32-33 °C after June 21st (Figure 2.6a). Leaf-air temperature differences (Figure 2.6b) ranged from -0.5 °C to -3.5 °C, and leaf to air VPD (Figure 2.6c), measured inside the LI-COR 6800 chamber, ranged from 1.2 to 2.2 kPa. The leaf temperatures noted throughout the growing season remained below high temperature thresholds shown to negatively impact cotton physiology (Hodges et al., 1993, Snider et al., 2010; Oosterhuis and Snider, 2011). Leaf-air temperatures exhibited a predictable response to VPD changes: low leaf to air VPD values corresponded to small leaf-air temperature differences, high leaf to air VPDs generated larger differences in canopy-air temperatures. This is in close agreement with previous reports on the canopy-air temperature response to VPD (Jackson et al., 1991; Chastain et al., 2016). As previously discussed in the statistical analysis section, in the humid South Georgia production environment the three investigated cotton cultivars did not exhibit any difference in stomatal conductance (and thus in their transpiration response to VPD) during the 2018 growing season and, as expected, this resulted in the same canopy-air temperature to VPD response for all the evaluated cultivars.

SmartCrop-based and Sentinel-based Crop Water Stress Indices

For SmartCrop™-derived canopy-air temperature differences to VPD, a strong, negative linear relationship was defined ($R^2 = 0.77$; $P < 0.001$). SmartCrop™-based well-watered baseline was calculated as: $T_c - T_a = 0.7823 - 2.0931 \text{ VPD}$ (Figure 2.7a). To identify a possible year-to-year change in SmartCrop™-derived well-watered baseline, the 2018 baseline was compared to the baseline previously defined by Chastain et al., 2016 ($T_c - T_a = 0.4404 - 1.7912 \text{ VPD}$). Idso CWSI values were calculated using both baselines and compared. The regression between the two different methods showed a strong positive relationship ($R^2 = 0.987$; $P < 0.001$; Figure 2.8), where Chastain et al. (2016) CWSI values were generally 10-15% higher than values calculated with the 2018 baseline ($\text{CWSI}_{2018} = 0.03186 + 0.8146 \text{ ChastainCWSI}$). Moreover, for Sentinel™-derived canopy-air temperature differences to VPD (well-watered baseline), a negative linear relationship was defined as well ($R^2 = 0.66$; $P < 0.001$). The Sentinel™-based well-watered baseline was calculated as: $T_c - T_a = -4.0627 - 2.5267 \text{ VPD}$ (Figure 2.7b).

During the cotton squaring period (first and second sampling dates), both SmartCrop™-based (Figure 2.11a) and Sentinel™-based (Figure 2.11b) CWSI averages were sensibly overestimating the real water status condition of the plants, defined as leaf water potential and gas exchange measurements, suggesting soil background effect could strongly affect CWSI calculations for both systems. After cotton squaring, all the different SmartCrop™-based CWSIs showed similar trends during the rest of the growing season. For Sentinel™-based CWSIs, all the energy balance approaches (Jones 1, Jones 2, and Monteith) tended to overestimate the real plant water status condition of the plots (Figure 2.11a) and the Idso CWSI seemed the only approach that agreed with the previously defined relationship between CWSI and Ψ_{PD} season-long averages for cotton in the Southeastern US (Chastain et al., 2016).

Canopy temperature was once again found to be a reliable indicator of crop water status, even in the Southeastern US where environmental conditions make the use of canopy temperature for water status detection challenging (Jones, 2004). The SmartCrop™-based well-watered baseline for the 2018 growing season showed CWSI values similar to those calculated using the Chastain et al. (2016) baseline, suggesting a general well-watered baseline could be used for the definition of a user-friendly IRT-based irrigation scheduling tool in the Southeast for several crops (Porter et al., 2015; Chastain et al., 2016). Season-long Ψ_{PD} and CWSI averages for the Sentinel™-based Idso CWSI and all the SmartCrop™-based CWSIs (data not shown) agreed with the CWSI- Ψ_{PD} relationship previously described by Chastain et al. (2016) for cotton; however, the lack of water stress during the season limited the possibility of comparison between the two models over comparable data ranges and further studies may be necessary to evaluate the Sentinel™-based CWSI response when drought stress is verified.

Sentinel CWSI vs Root Zone Soil Water Deficit comparison

Between Sentinel™-derived Idso CWSI and 100% ET treatment-Root Zone Soil Water Deficit, a linear relationship was observed ($R^2 = 0.59$; $P < 0.01$). A similar response was defined between the 125% ET treatment CWSI ($R^2 = 0.599$) and RZSWD (data not shown). The Cotton App water balance method was once again shown to be a reliable indicator of crop water status applicable for irrigation scheduling (Vellidis et al., 2016). The Cotton App has been shown to produce higher yields and better irrigation WUE, when compared to conventional water balance irrigation approaches as the UGA Checkbook method (Migliaccio et al., 2016). One of the objectives of this study was to compare the novel camera-based CWSI to well-established crop water status estimates. The strong relationship between Sentinel™ camera-derived CWSI and

RZSWD indicates that thermal imagery may be a sensitive indicator of the onset of soil water depletion, even before negative physiological consequences are observed. This relationship should be tested further over a broader range of soil water deficit conditions, such as those observed by Meeks et al. (2017).

Sentinel vs SmartCrop Idso CWSI comparison

Finally, SmartCrop™-derived Idso CWSI averages were plotted against Sentinel™-derived Idso CWSI averages calculated on the same sampling dates. Sentinel™ CWSI was considered the dependent variable and SmartCrop™ CWSI the independent variable. A strong, linear relationship was found between Sentinel™-based and SmartCrop™-based values ($R^2 = 0.84$; $P < 0.001$; Figure 2.10). The main objective of this study was to investigate the accuracy of the Sentinel thermal imaging system in estimating canopy temperatures, and to validate the system by means of well-established methods shown to be strong indicators of plant water stress. The Sentinel™ camera demonstrated a strong linear relationship with SmartCrop™-based Crop Water Stress Index values, suggesting the system could be considered an accurate indicator of canopy temperatures and used for CWSI calculations in the humid Southeastern US. Moreover, the camera exhibited a consistent accuracy pattern in estimating canopy temperatures when increasing the distance between the camera position and the investigated plots (R^2 ranging from 0.94 for the closest plots at 65 m from the camera to 0.77 at 150-170 m from the camera, data not shown).

In conclusion, being able to utilize CWSIs calculated using this novel thermal imagery approach will allow the definition of IMZ boundaries and irrigation thresholds that could be modified on a daily basis, considering dynamic changes in crop water status as the season

progresses. This allows farmers to apply water only when and where the crop needs it, providing the potential of increasing cotton yields and WUE at the whole-field scale (Chastain et al., 2016; Liakos et al., 2017).

Dry matter accumulation, IPAR_{TOTAL}, and RUE

For the 2018 growing season, the total amount of solar radiation from planting to defoliation was 2621.51 MJ m⁻². Above-ground dry weight (DW), total solar radiation, average IPAR, IPAR_{total} and RUE data are shown in Table 2.2. Average IPAR ranged from a minimum of 0.654 for the Rainfed treatment to a maximum of 0.669 for the 100% ET treatment. IPAR_{tot}, calculated as total solar radiation x 0.45 x average IPAR, ranged between 771.5 (Rainfed) to 789.3 MJ m⁻² (100% ET treatment). Dry weight, estimated using a 0.91 m-row spacing for cotton, ranged from 911.7 g m⁻² (Rainfed) to 1062.2 g m⁻² (125% ET treatment). Radiation Use Efficiency, calculated as DW/IPAR_{tot}, resulted in values between 1.189 (Rainfed) and 1.359 g MJ⁻¹ (125% ET treatment). Even if the irrigation treatments did not show any significant difference, IPAR_{tot}, DW and RUE values were generally higher for irrigated (100% ET and 125% ET treatments) vs non-irrigated cotton (Rainfed). Average IPAR, DW and RUE agreed closely with values previously reported in several published works for field-grown cotton (Rosenthal and Gerik, 1991; Sadras, 1996; Milroy and Bange, 2003; Yeates et al., 2010).

References:

- Alchanatis, V., Cohen, Y., Cohen, S., Moller, M., Sprinstin, M., Meron, M., ... & Sela, E. (2010). Evaluation of different approaches for estimating and mapping crop water status in cotton with thermal imaging. *Precision Agriculture*, 11(1), 27-41.
- Allen, R. G., Pereira, L. S., Raes, D., & Smith, M. (1998). *Crop evapotranspiration-Guidelines for computing crop water requirements-FAO Irrigation and drainage paper 56*. Fao, Rome, 300(9), D05109.
- Baker, J. T., Gitz, D. C., Payton, P., Wanjura, D. F., & Upchurch, D. R. (2007). Using leaf gas exchange to quantify drought in cotton irrigated based on canopy temperature measurements. *Agronomy Journal*, 99(3), 637-644.
- Bednarz, C. W., Hook, J., Yager, R., Cromer, S., Cook, D., & Griner, I. (2002). Cotton crop water use and irrigation scheduling. AS Culpepper et al.(ed.), 61-64.
- Chastain, D. R., Snider, J. L., Collins, G. D., Perry, C. D., Whitaker, J., & Byrd, S. A. (2014). Water deficit in field-grown *Gossypium hirsutum* primarily limits net photosynthesis by decreasing stomatal conductance, increasing photorespiration, and increasing the ratio of dark respiration to gross photosynthesis. *Journal of Plant Physiology*, 171(17), 1576-1585.
- Chastain, D. R., Snider, J. L., Collins, G. D., Perry, C. D., Whitaker, J., Byrd, S. A., ... & Porter, W. M. (2016). Irrigation scheduling using predawn leaf water potential improves water productivity in drip-irrigated cotton. *Crop Science*, 56(6), 3185-3195.
- Cohen, Y., Alchanatis, V., Meron, M., Saranga, Y., & Tsipris, J. (2005). Estimation of leaf water potential by thermal imagery and spatial analysis. *Journal of experimental botany*, 56(417), 1843-1852.
- Cohen, Y., Alchanatis, V., Saranga, Y., Rosenberg, O., Sela, E., & Bosak, A. (2017). Mapping water status based on aerial thermal imagery: comparison of methodologies for upscaling from a single leaf to commercial fields. *Precision Agriculture*, 18(5), 801-822.
- Constable, G. A., & Oosterhuis, D. M. (2010). Temporal dynamics of cotton leaves and canopies. In *Physiology of Cotton* (pp. 72-79). Springer, Dordrecht.
- Earl, H. J., & Davis, R. F. (2003). Effect of drought stress on leaf and whole canopy radiation use efficiency and yield of maize. *Agronomy journal*, 95(3), 688-696.
- Flash, I. (2014). Can plant-based moisture sensing improve irrigation scheduling and water use efficiency? Practical cotton remote sensing project, Israel 2013. In *Proceedings of the 2014 Beltwide Cotton Conferences (USA)*.

- Hodges, H. F., Reddy, K. R., McKinion, J. M., & Reddy, V. R. (1993). Temperature effects on cotton. *Bulletin (USA)*.
- Hsiao, T. C. (1973). Plant responses to water stress. *Annual review of plant physiology*, 24(1), 519-570.
- Hu, W., Snider, J. L., Wang, H., Zhou, Z., Chastain, D. R., Whitaker, J., ... & Bourland, F. M. (2018). Water-induced variation in yield and quality can be explained by altered yield component contributions in field-grown cotton. *Field Crops Research*, 224, 139-147.
- Idso, S. B., Jackson, R. D., Pinter Jr, P. J., Reginato, R. J., & Hatfield, J. L. (1981). Normalizing the stress-degree-day parameter for environmental variability. *Agricultural Meteorology*, 24, 45-55.
- Jackson, S. H. (1991). Relationships between normalized leaf water potential and crop water stress index values for acala cotton. *Agricultural Water Management*, 20(2), 109-118.
- Jones, H. G. (1999). Use of infrared thermometry for estimation of stomatal conductance as a possible aid to irrigation scheduling. *Agricultural and forest meteorology*, 95(3), 139-149.
- Jones, H. G. (2004). Irrigation scheduling: advantages and pitfalls of plant-based methods. *Journal of experimental botany*, 55(407), 2427-2436.
- Jones, H. G., Stoll, M., Santos, T., Sousa, C. D., Chaves, M. M., & Grant, O. M. (2002). Use of infrared thermography for monitoring stomatal closure in the field: application to grapevine. *Journal of Experimental Botany*, 53(378), 2249-2260.
- Kiniry, J. R., Jones, C. A., O'toole, J. C., Blanchet, R., Cabelguenne, M., & Spanel, D. A. (1989). Radiation-use efficiency in biomass accumulation prior to grain-filling for five grain-crop species. *Field Crops Research*, 20(1), 51-64.
- Krieg, D. R., & Sung, J. F. M. (1986). Source-sink relations as affected by water stress during boll development. *Cotton physiology*, 7377.
- Liakos, V., Porter, W., Liang, X., Tucker, M. A., McLendon, A., & Vellidis, G. (2017). Dynamic Variable Rate Irrigation—A Tool for Greatly Improving Water Use Efficiency. *Advances in Animal Biosciences*, 8(2), 557-563.
- Loka, D. A., & Oosterhuis, D. M. (2012). Water stress and reproductive development in cotton. *Flowering and Fruiting in Cotton*. Cordova: The Cotton Foundation, 51-58.
- Meek, D. W., Hatfield, J. L., Howell, T. A., Idso, S. B., & Reginato, R. J. (1984). A Generalized Relationship between Photosynthetically Active Radiation and Solar Radiation 1. *Agronomy journal*, 76(6), 939-945.

- Meeks, C. D., Snider, J. L., Porter, W. M., Vellidis, G., Hawkins, G., & Rowland, D. (2017). Assessing the Utility of Primed Acclimation for Improving Water Savings in Cotton using a Sensor-Based Irrigation Scheduling System. *Crop Science*, 57(4), 2117-2129.
- Milroy, S. P., & Bange, M. P. (2003). Nitrogen and light responses of cotton photosynthesis and implications for crop growth. *Crop science*, 43(3), 904-913.
- Molz, F. J., & Klepper, B. (1973). On the Mechanism of Water-Stress-Induced Stem Deformation 1. *Agronomy Journal*, 65(2), 304-306.
- Monteith, J. L., & Unsworth, M. H. (1990). *Principles of environmental physics*. London: Edward Arnold.
- Monteith, J. L. (1965). Radiation and crops. *Experimental Agriculture*, 1(4), 241-251.
- Forti, R., & Henrard., M. (2016) Eurostat, Agriculture, forestry, and fishery statistics 2016 edition. Eurostat. Retrieved from <https://ec.europa.eu/eurostat/documents/3217494/7777899/KS-FK-16-001-EN-N.pdf/cae3c56f-53e2-404a-9e9e-fb5f57ab49e3>
- Oosterhuis, D. M., & Snider, J. L. (2011). High temperature stress on floral development and yield of cotton. *Stress physiology in cotton*, 7, 1-24.
- Oosterhuis, D. M., & Wullschleger, S. D. (1988). Carbon partitioning and photosynthetic efficiency during boll development. In *Proceedings-Beltwide Cotton Production Research Conferences (USA)*.
- Pettigrew, W. T. (2004). Physiological consequences of moisture deficit stress in cotton. *Crop Science*, 44(4), 1265-1272.
- Porter, W. M., Snider, J. L., Perry, C. D., Monfort, W. S., & Vellidis, G. (2015). SmartCrop® Sensors for Predicting Irrigation Requirements for Peanut in the Southeast. In *2015 ASABE Annual International Meeting* (p. 1). American Society of Agricultural and Biological Engineers.
- Rosenthal, W. D., & Gerik, T. J. (1991). Radiation use efficiency among cotton cultivars. *Agronomy Journal*, 83(4), 655-658.
- Sadras, V. O. (1996). Cotton responses to simulated insect damage: radiation-use efficiency, canopy architecture and leaf nitrogen content as affected by loss of reproductive organs. *Field Crops Research*, 48(2-3), 199-208.
- Sharp, R. E., Poroyko, V., Hejlek, L. G., Spollen, W. G., Springer, G. K., Bohnert, H. J., & Nguyen, H. T. (2004). Root growth maintenance during water deficits: physiology to functional genomics. *Journal of experimental botany*, 55(407), 2343-2351.

Snider, J. L., Oosterhuis, D. M., & Kawakami, E. M. (2010). Genotypic differences in thermotolerance are dependent upon prestress capacity for antioxidant protection of the photosynthetic apparatus in *Gossypium hirsutum*. *Physiologia plantarum*, 138(3), 268-277.

Snider, J.L. & Oosterhuis D. M. (2015). *Physiology. Cotton* 2nd edition (pp 339-400). D. Fang and R. Percy. Madison, WI. ASA-CSSA-SSSA.

Snider, J.L. and Chastain D.R. (2016) *Plant-Based Irrigation Scheduling. Linking Physiology to Management* (pp 97-116). Snider J.L. and Oosterhuis D.M. The Cotton Foundation, Cordova, TN.

USDA National Agricultural Statistics Service. (2014). *Farm and Ranch Irrigation Survey 2013*. Retrieved from https://www.nass.usda.gov/Publications/AgCensus/2012/Online_Resources/Farm_and_Ranch_Irrigation_Survey/fris13.pdf

Vellidis, G., Liakos, V., Perry, C., Tucker, M., Collins, G., Snider, J., ... & Rowland, D. (2014). A smartphone app for scheduling irrigation on cotton. In *Proceedings of the 2014 Beltwide Cotton Conference*, New Orleans, LA, National Cotton Council, Memphis, TN.

Vellidis, G., Liakos, V., Porter, W., Tucker, M., & Liang, X. (2016). *A Dynamic Variable Rate Irrigation Control System*. St. Louis, Missouri: Academic Publishers.

Vories, E. D., Teague, T., Greene, J., Stewart, J., Clawson, E., Pringle, L., & Phipps, B. (2006). Determining the optimum timing for the final irrigation on mid-South cotton. In *Proceedings National Cotton Council Beltwide Cotton Conference* (pp. 516-521).

Whitaker, J., Culpepper, S., Freeman, M., Harris, G., Kemerait, B., Perry, C., ... & Smith, A. (2018). *Georgia Cotton Production Guide*. Cooperative Extension, University of Georgia.

Yeates, S. J., Constable, G. A., & McCumstie, T. (2010). Irrigated cotton in the tropical dry season. II: Biomass accumulation, partitioning and RUE. *Field Crops Research*, 116(3), 290-299.

Figure Captions

Fig. 2.1 Daily Maximum (solid line) and Minimum (dotted line) air temperature and precipitation (vertical bars) during the 2018 growing season from the GAEMN weather station located at the Stripling Irrigation Research Park in Camilla, GA.

Fig. 2.2 Daily deep soil water tension weighted averages (solid line) and root zone soil water deficit (dotted line) observed during the 2018 growing season in Camilla, GA for the 100% ET irrigation treatment. Deep soil water tension weighted averages were calculated as: $0.5 * \text{SWT at 15cm} + 0.3 * \text{SWT at 30cm} + 0.2 * \text{SWT at 45cm}$.

Fig. 2.3 Pre-dawn (A) and Midday (B) leaf water potential for Rainfed (black circles), 100% ET (white circles), and 125% ET (black triangles) irrigation treatments during the 2018 growing season in Camilla, GA. Data are shown as means \pm standard errors ($n = 18$).

Fig. 2.4 Average height (A), mainstem nodes (B), and canopy interception of photosynthetically active radiation (IPAR; C) for Rainfed (black circles), 100% ET (white circles), and 125% ET (black triangles) irrigation treatments during the 2018 growing season in Camilla, GA. Data are shown as mean \pm standard errors ($n = 18$). For plant height and mainstem nodes, five plants per plots were measured to provide a plot representative value.

Fig. 2.5 Net photosynthesis (A), stomatal conductance to water vapor (B), and intrinsic water use efficiency (C) for Rainfed (black circles), 100% ET (white circles), and 125% ET (black triangles) irrigation treatments during the 2018 growing season in Camilla, GA. Data are shown as means \pm standard errors ($n = 18$).

Fig. 2.6 Leaf temperature (A), leaf – air temperature (B), and leaf to air vapor pressure deficit (C) collected using LI-COR LI-6800 portable photosynthesis system for Rainfed (black circles), 100% ET (white circles), and 125% ET (black triangles) irrigation treatments during the 2018 growing season in Camilla, GA. Data are shown as means \pm standard errors (n = 18).

Fig. 2.7 Canopy – Air temperature differences versus vapor pressure deficit (VPD) for well-watered cotton plots (125% ET treatment) located in Camilla, GA. Temperature differences were calculated for both SmartCrop™ infrared thermometers (A) and the Sentinel™ thermal camera (B). Data were collected for a month-long period during flowering (6/26/2018 – 7/26/2018), filtered to include only values between 1200-1400h, on days where solar radiation was greater than 600 W m^{-2} (Chastain et al., 2016), and averaged for each date prior to regression (n = 18 for Sentinel™ data, n = 9 for SmartCrop™ data).

Fig. 2.8 Chastain et al (2016) SmartCrop baseline-derived Idso CWSI vs 2018 SmartCrop baseline-derived Idso CWSI graph. Data were averaged for all the sampling dates and all the irrigation treatments (n = 9).

Fig. 2.9 Relationship between Sentinel-derived Idso CWSI and Root Zone Soil Water Deficit (RZSWD). CWSI values were averaged for all the different irrigation treatments on all the sampling dates (n = 9), RZSWD was calculated using the previously described soil water deficit calculation sheet.

Fig. 2.10 Relationship between Sentinel™-based Crop Water Stress Index (CWSI) and SmartCrop™-based Crop Water Stress Index (CWSI) values calculated on each single sampling date for three different irrigation treatments. CWSI was calculated using the Idso et al. (1981)

formula. Two different well-watered baselines were used to calculate CWSI values for the two different systems (Figure 2.7). Each data point represents a combination between a Sentinel™ CWSI average (n = 18) and a SmartCrop™ CWSI average (n = 9).

Fig. 2.11 Different Crop Water Stress Indices calculated using canopy temperatures collected using SmartCrop™ (A) infrared thermometer and the Sentinel™ (B) thermal camera during the 2018 growing season in Camilla, GA. Idso CWSI was calculated using the procedure shown in Idso et al. (1981); Jones1 CWSI was calculated using the Jones (1999) energy balance equation for both dry and wet baselines; Jones2 CWSI was calculated using $T_{air} + 5^{\circ}\text{C}$ as dry baseline and the Jones (1999) energy balance equation as wet baseline; Monteith CWSI was calculated using $T_{air} + 5^{\circ}\text{C}$ as dry baseline and the Monteith and Unsworth (1990) energy balance equation as wet baseline. Each group of bars represents averages calculated considering all the irrigation treatments for every sampling date (n = 54 for Sentinel CWSI, n = 27 for SmartCrop CWSI).

Table 2.1 Irrigation + Rainfall amounts (in centimeters) and number of irrigation events for the three different irrigation treatments (Rainfall, 100% ET, and 125% ET) from planting to defoliation during the 2018 growing season.

Treatment	Rainfall [cm]	Irrigation [cm]	Irrigation Events	Rainfall + Irrigation [cm]
Rainfed	80.3	0.0	0	80.3
100% ET	80.3	21.1	12	101.4
125% ET	80.3	22.1	12	102.4

Table 2.2 Total solar radiation, average canopy interception of photosynthetically active radiation (IPAR), total IPAR from planting to defoliation (IPAR_{total}), dry weight (DW), and radiation use efficiency (RUE) for the three irrigation treatments (Rainfall, 100% ET, and 125% ET) during the 2018 growing season. Data are presented as means \pm SE (n = 18). For a given parameter, different letters indicate the values are significantly different (Fisher's LSD, P < 0.05).

Irrigation Treatment	Total Solar Radiation [MJ m ⁻²]	Average IPAR	IPAR _{total} [MJ m ⁻²]	DW [g m ⁻²]	RUE [g MJ ⁻¹]
Rainfed		0.654 \pm 0.019 a	771.5 \pm 22.8 a	911.7 \pm 42.2 a	1.189 \pm 0.049 a
100% ET	2621.51	0.669 \pm 0.010 a	789.3 \pm 12.3 a	969.3 \pm 49.6 a	1.219 \pm 0.049 a
125% ET		0.664 \pm 0.010 a	783.1 \pm 11.6 a	1062.2 \pm 47.0 a	1.359 \pm 0.062 a

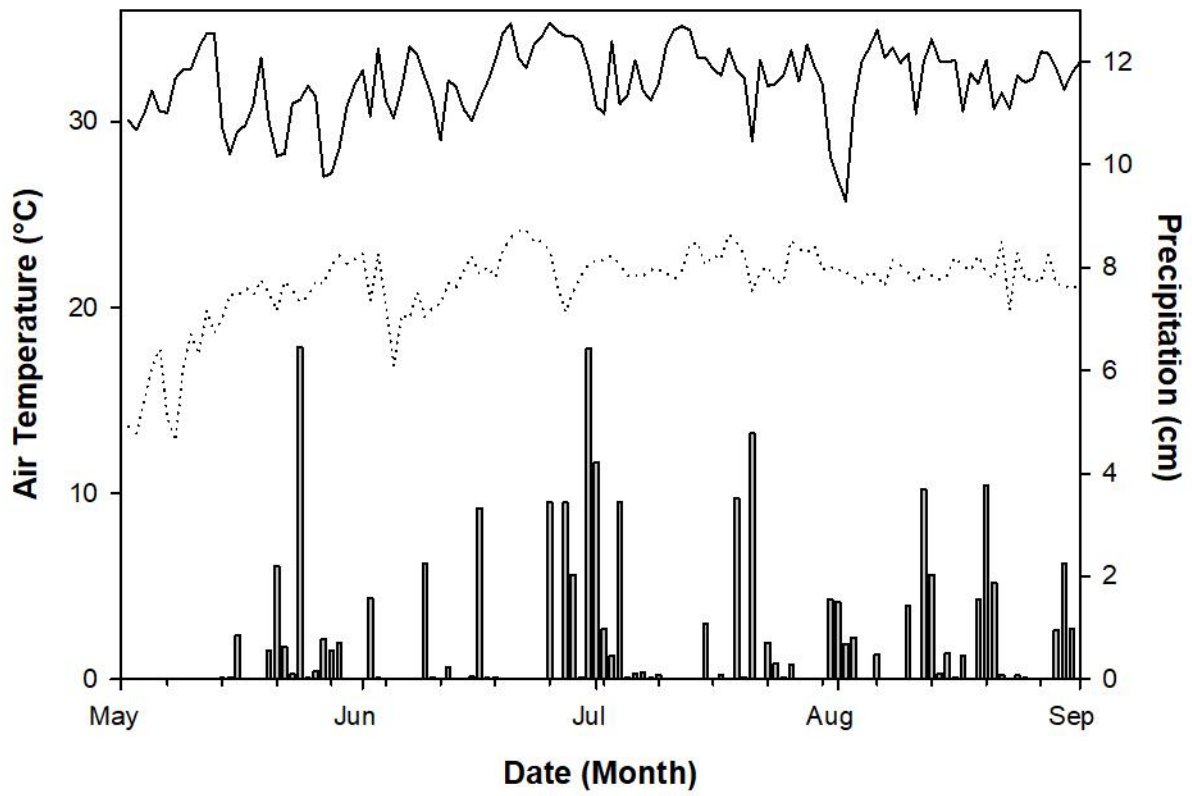


Figure 2.1

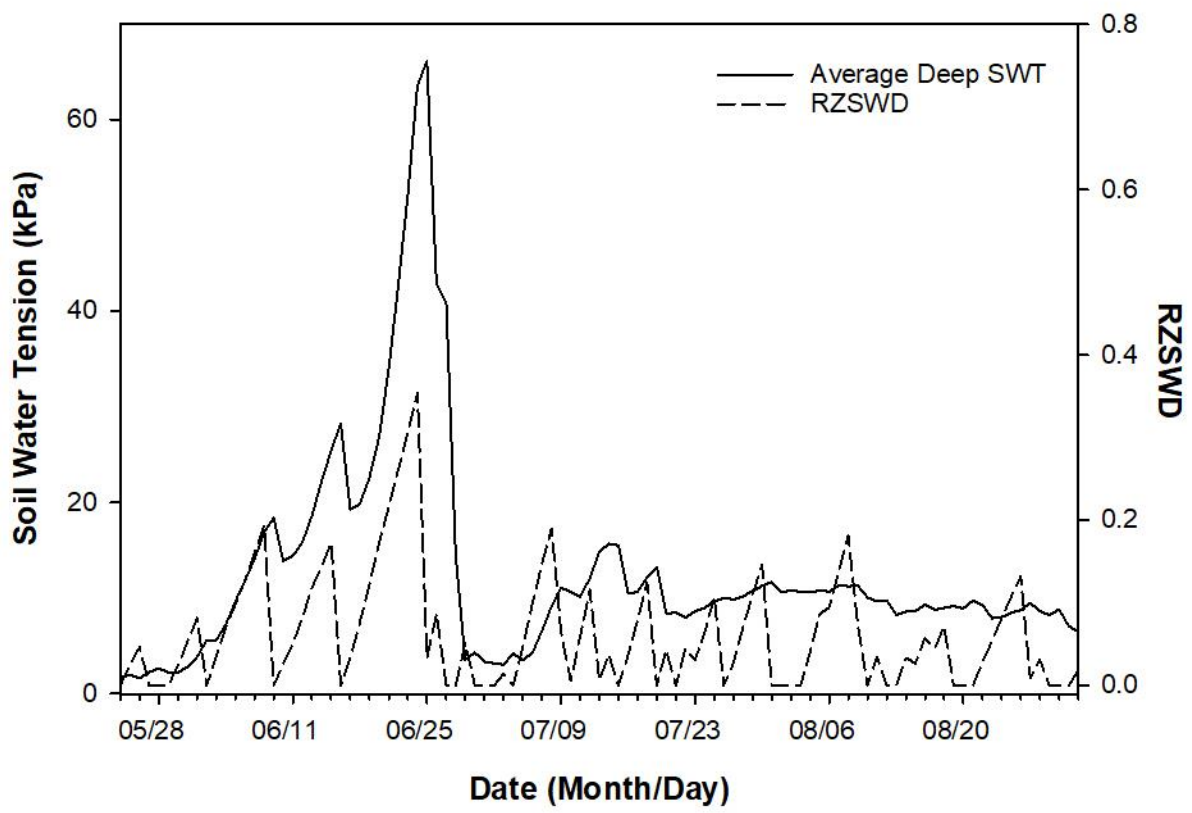


Figure 2.2

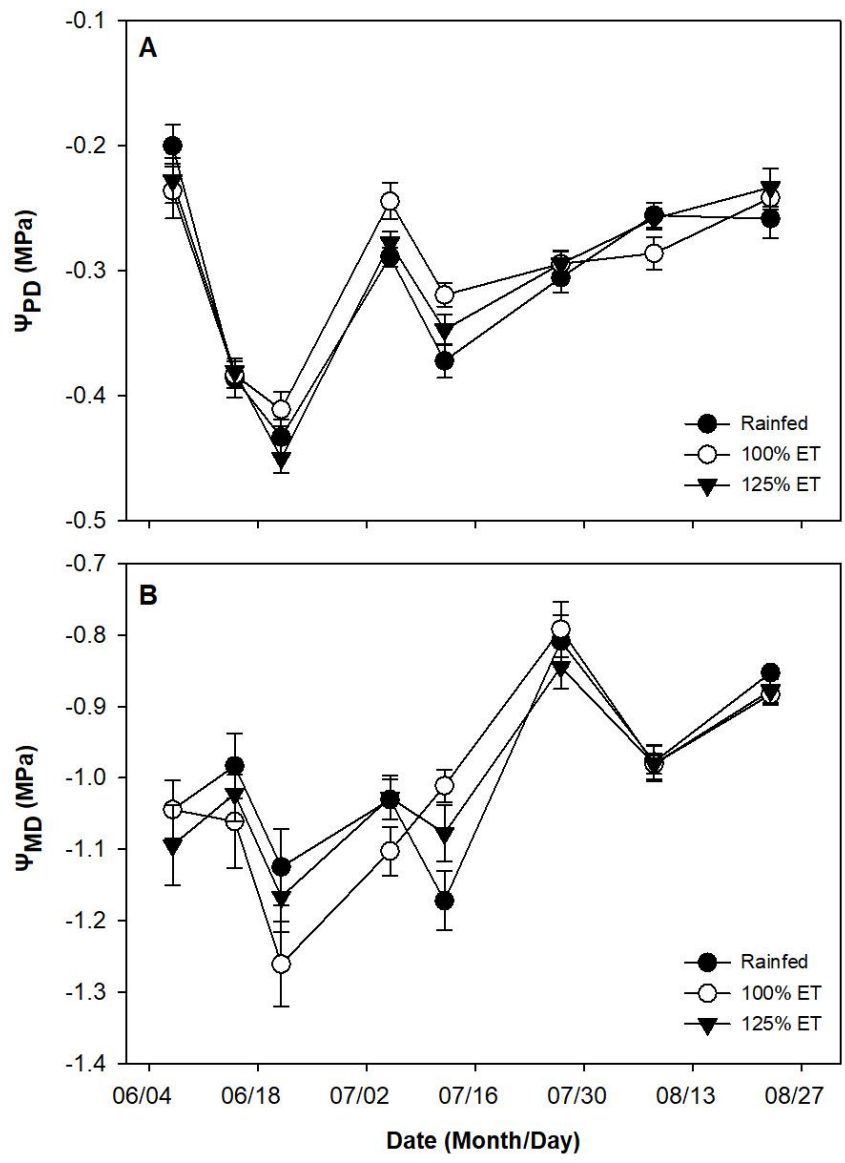


Figure 2.3

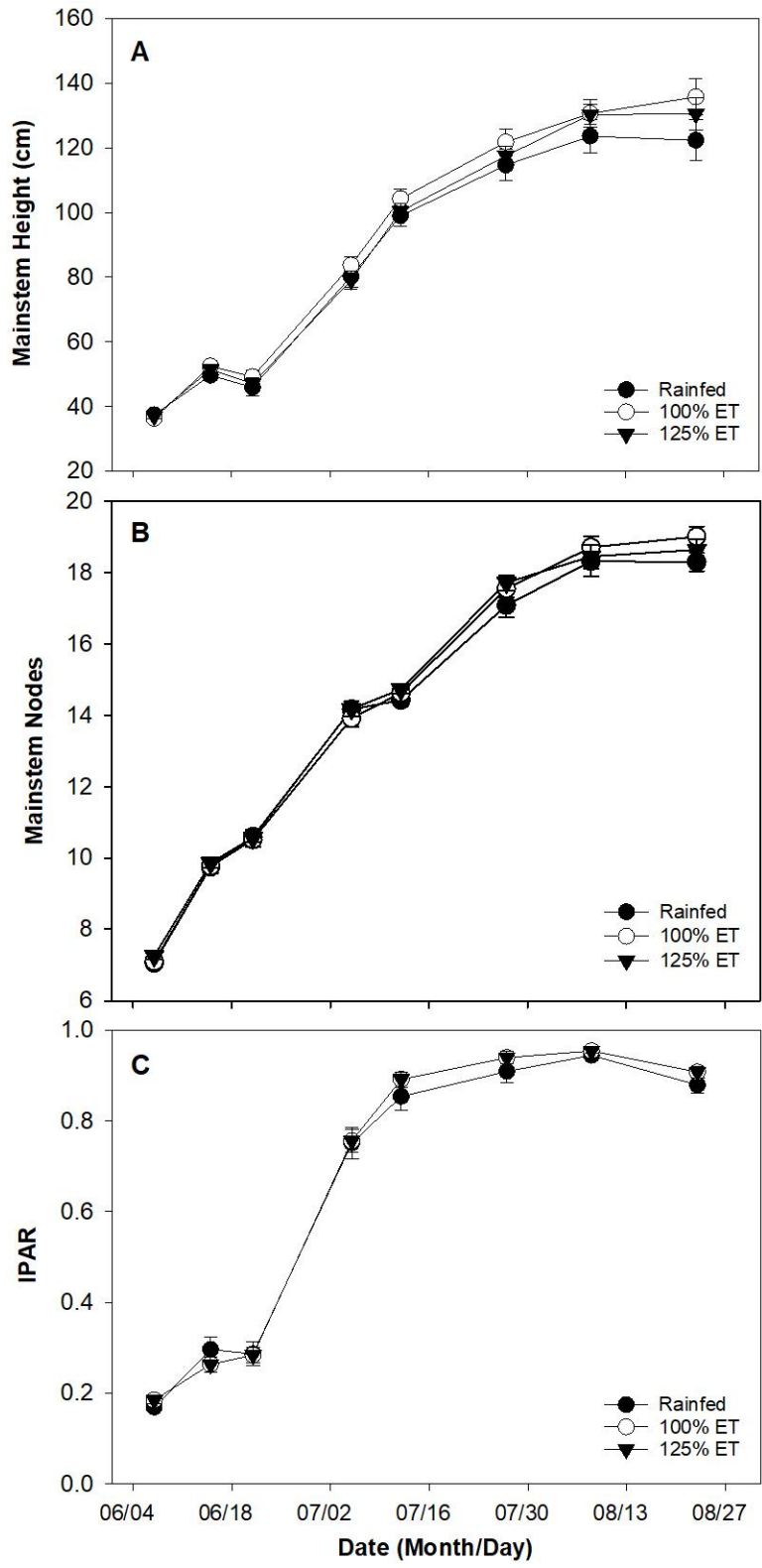


Figure 2.4

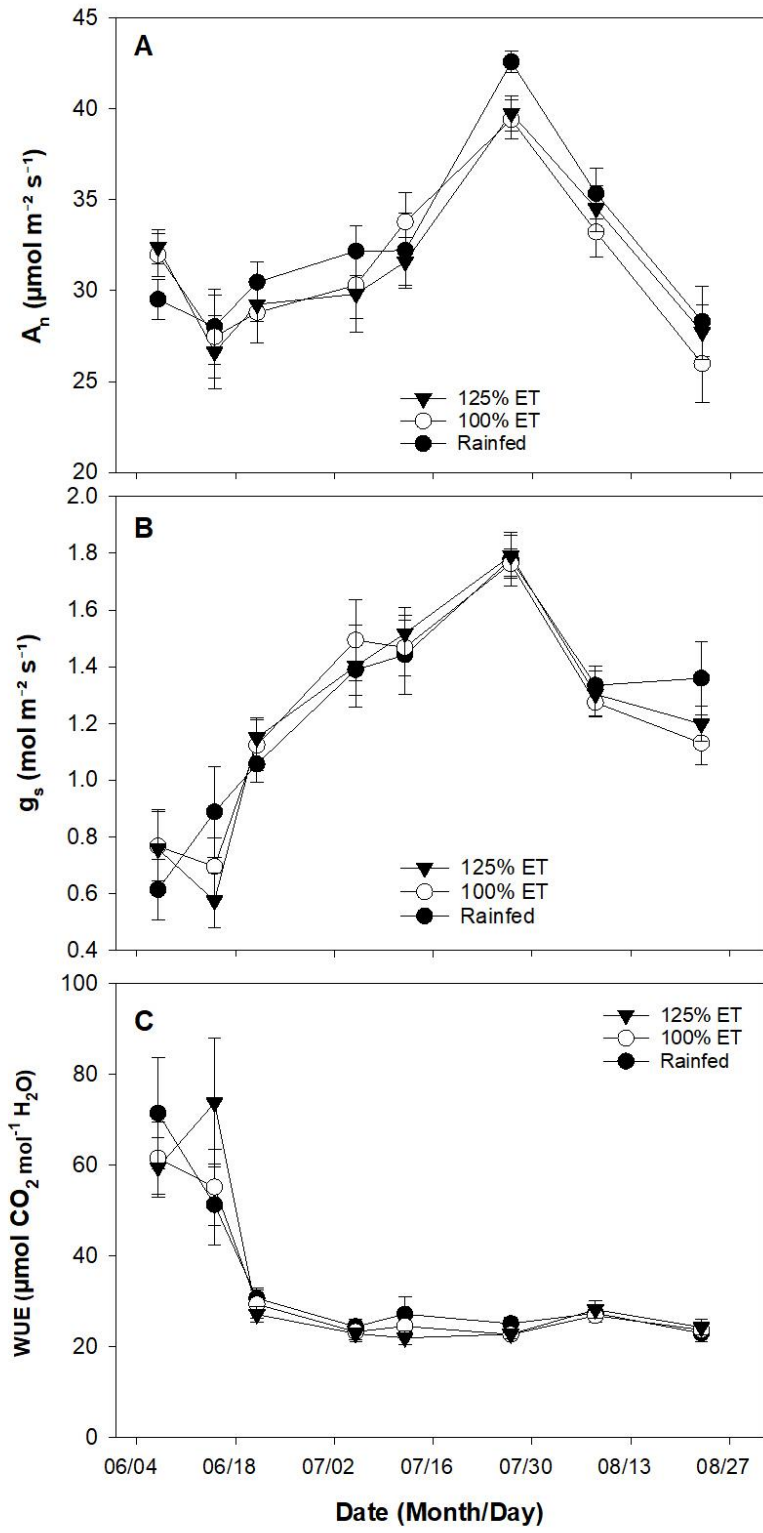


Figure 2.5

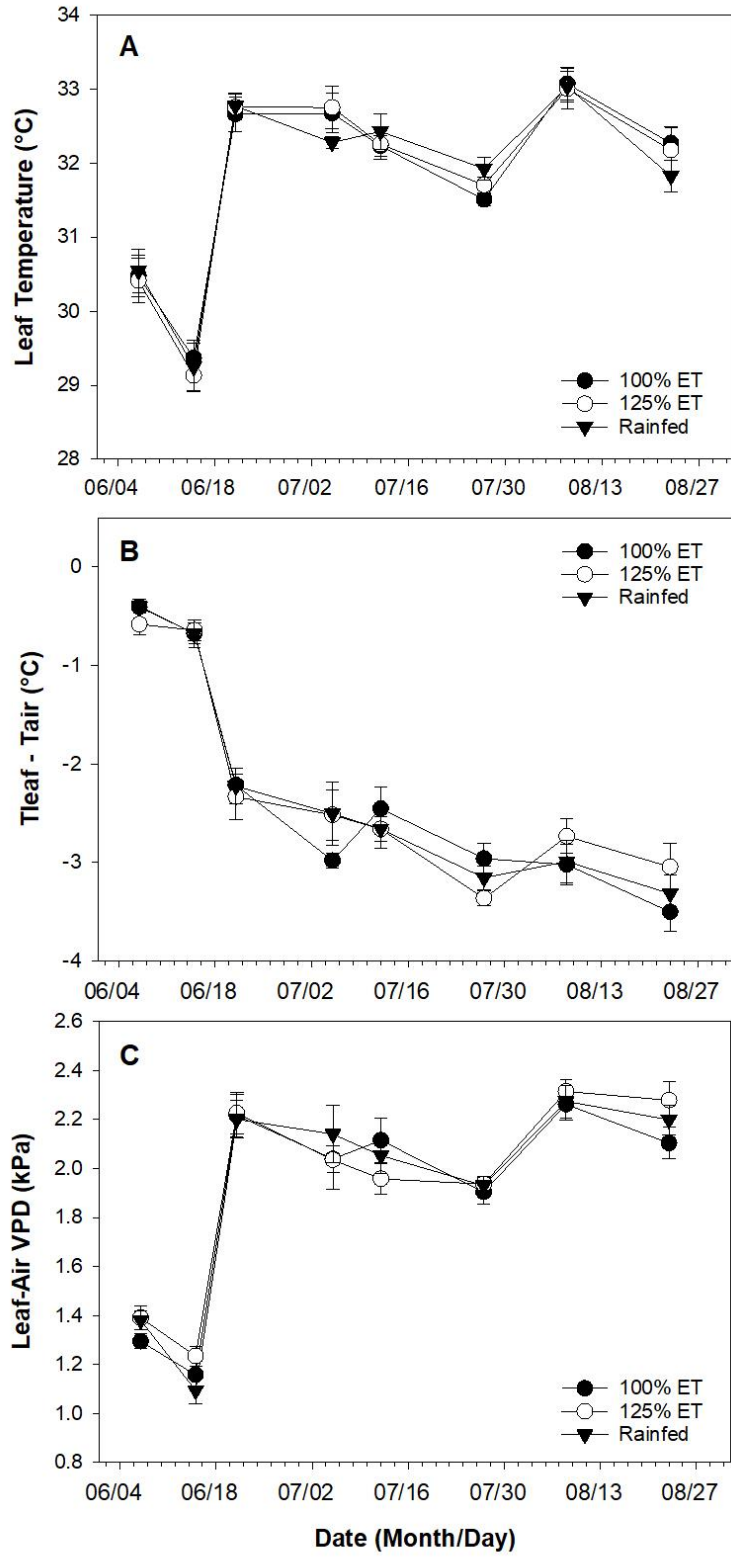


Figure 2.6

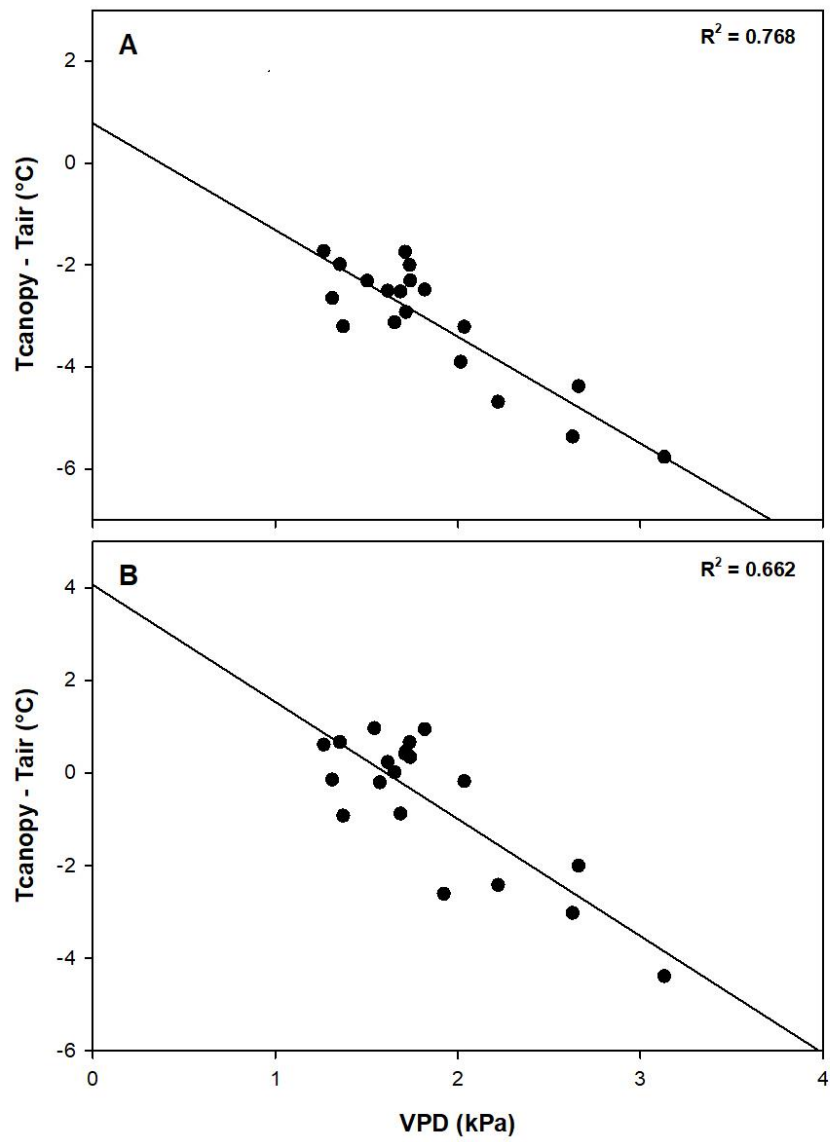


Figure 2.7

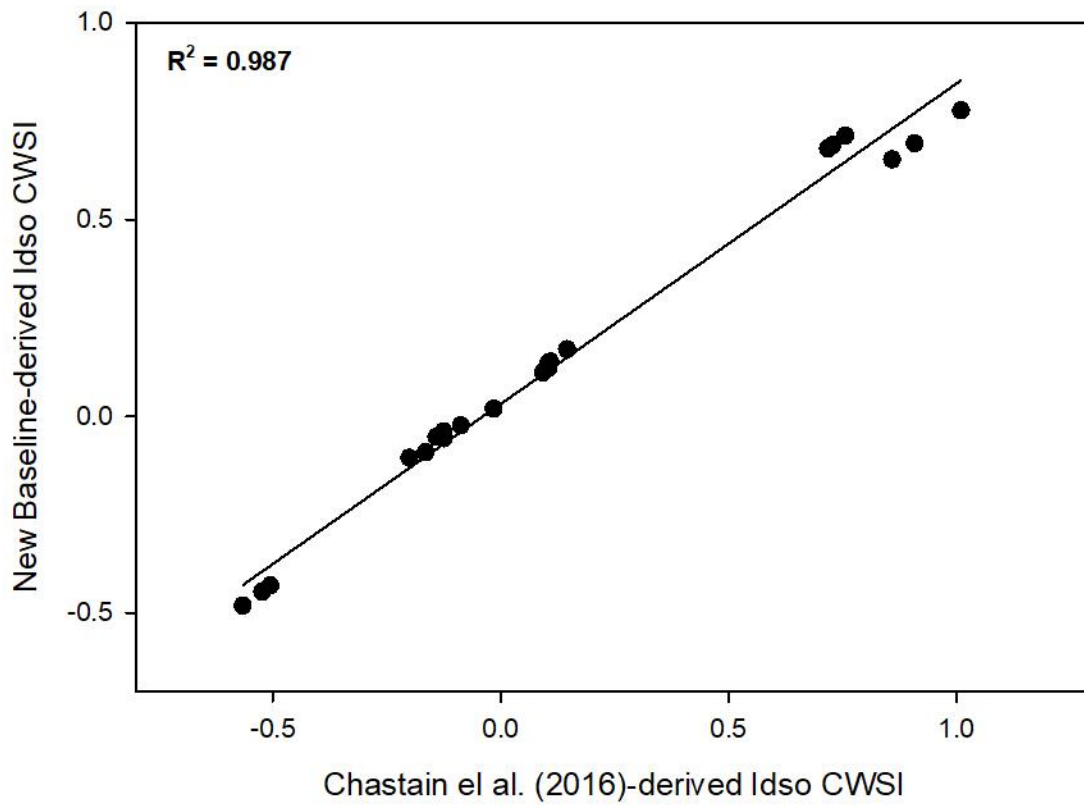


Figure 2.8

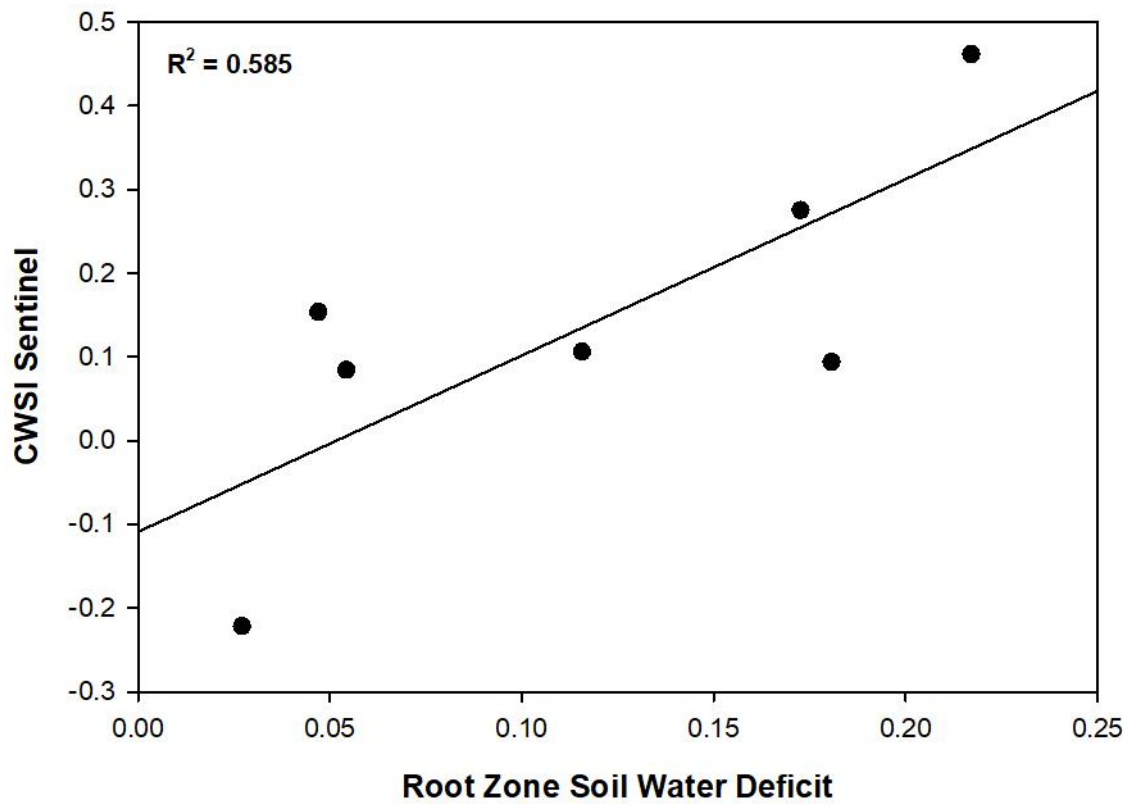


Figure 2.9

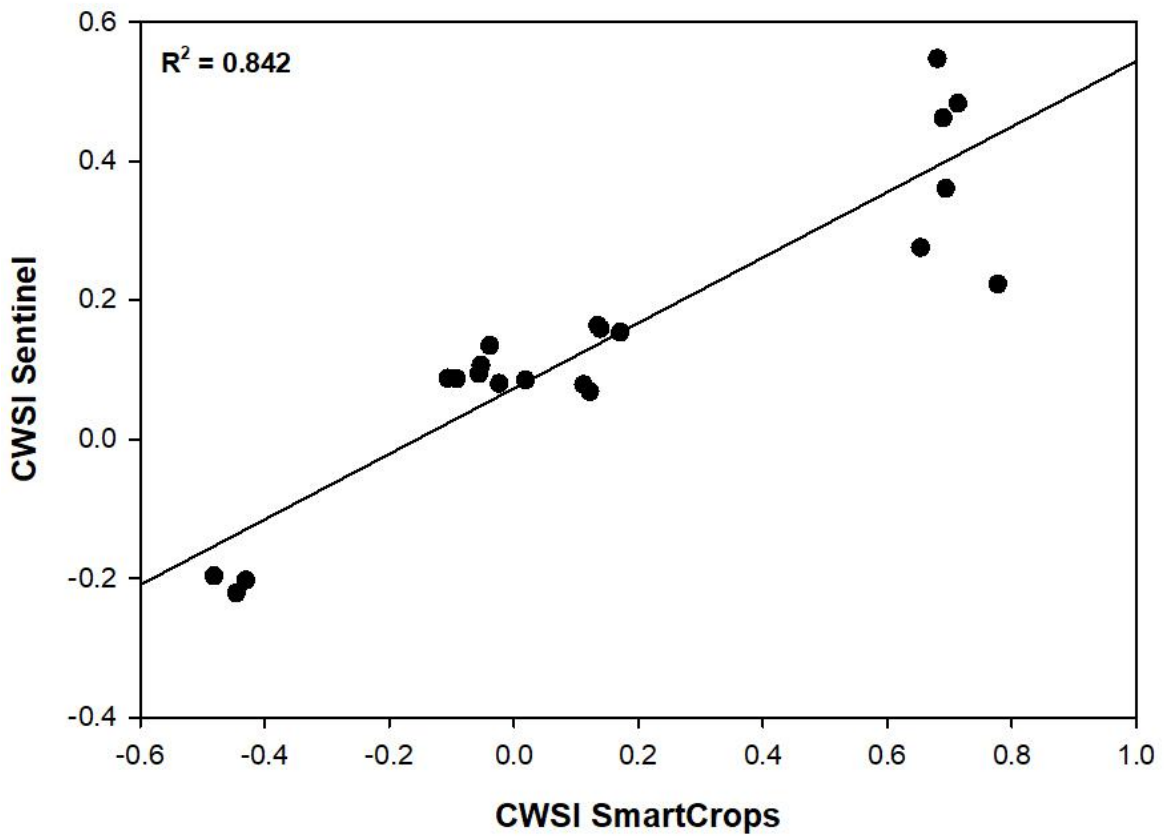


Figure 2.10

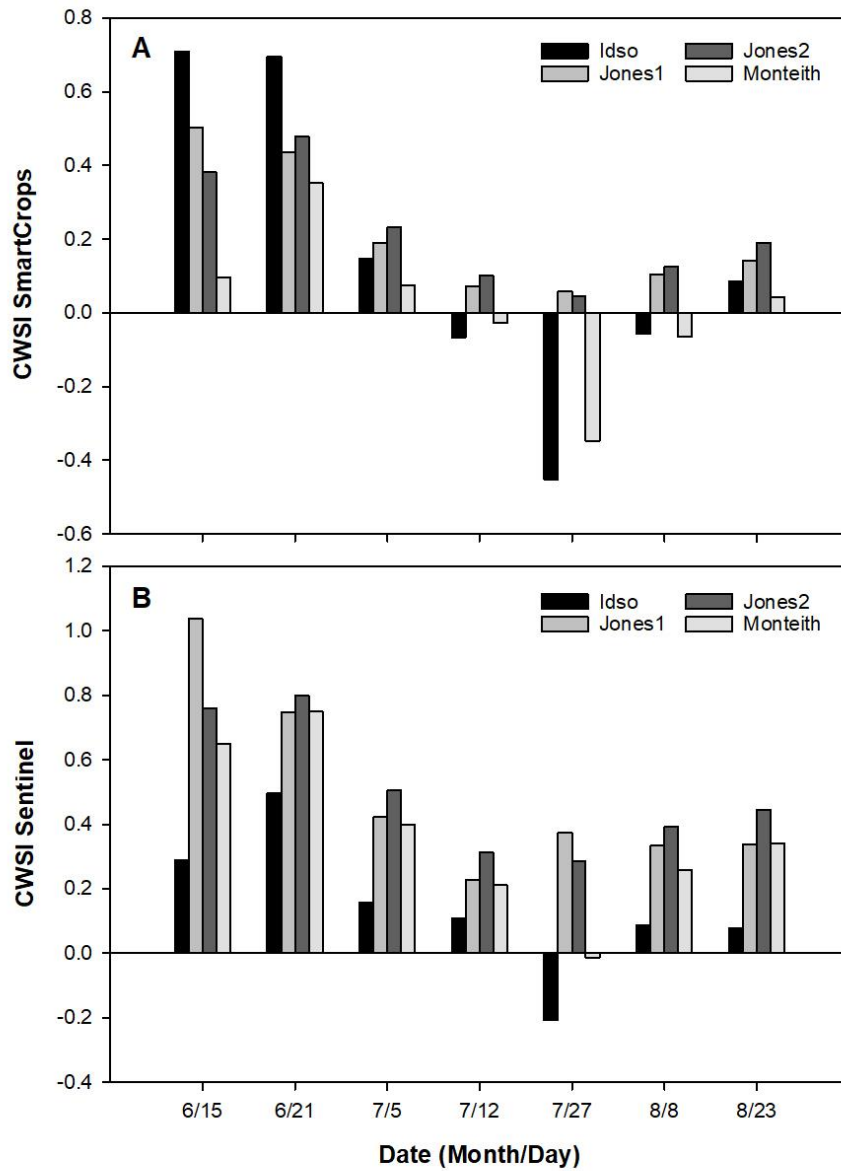


Figure 2.11

CHAPTER 3

CONCLUSION

In this study, the research objectives were (1) to validate a novel thermal camera system using well-established crop water status sensing methods and (2) to calculate the previously discussed Crop Water Stress Indices (CWSIs) from camera-derived canopy temperatures and relate them to established infrared thermometer (IRT)-based CWSIs and crop physiological responses.

During the 2018 growing season, no significant cultivar, irrigation or cultivar by irrigation interaction effects were observed for any physiological parameter on any given date, including predawn (Ψ_{PD}), and midday (Ψ_{MD}) leaf water potential, cotton growth (mainstem height, nodes and IPAR), or single-leaf gas exchange (net photosynthesis A_N , midday stomatal conductance g_s , and intrinsic water use efficiency $iWUE$). For SmartCrop™ IRTs, a linear, well-watered baseline response of canopy – air temperature versus vapor pressure deficit (VPD) was defined for the 2018 season ($R^2 = 0.77$), and this response as well as the CWSIs calculated from it, were comparable to a previous report by Chastain et al. (2016). This suggests a general well-watered baseline could be defined for cotton in the Southeastern US. For the novel thermal camera (Sentinel™) approach, a well-watered baseline was defined as well ($R^2 = 0.66$), and Sentinel™-based CWSI was found to agree with in-field IRT-based CWSI values ($R^2 = 0.84$) and root zone soil water deficits ($R^2 = 0.59$). Moreover, a strong relationship between the Sentinel™ CWSI estimation and in-field, IRT estimation was maintained even increasing the distance from the camera position up to 170 meters. However, defining a relationship between Sentinel™-based CWSI and leaf water potential was

not possible because of the limited drought stress events observed during the entire sampling period. Therefore, the four different CWSIs (Idso, Jones1, Jones2 and Monteith) calculated using both IRTs and Sentinel™ need further evaluation to define the best wet and dry baseline combination for CWSI calculations.

It was concluded that the Sentinel™ camera estimates of crop water status agreed closely with well-established method for assessing crop water status, even under soil water deficits insufficient to appreciably affect physiological processes. Thus, the aforementioned system could be deployed to capture the onset of drought to define canopy temperature-based transient irrigation management zones before negative physiological consequences are observed.